APPLICATION OF ANALYTICAL CENTRIFUGAL-PUMP PERFORMANCE MODELS IN TWO-PHASE FLOW

by

JAMES EDWARD KORENCHAN

S.B.M.E., Illinois Institute of Technology
(1982)

SUBMITTED TO THE DEPARTMENT OF MECHANICAL ENGINEERING IN PARTIAL FULFILLMENT OF THE REQUIREMENTS FOR THE DEGREE OF

MASTER OF SCIENCE

at the

MASSACHUSETTS INSTITUTE OF TECHNOLOGY

August 1984

Signature of Author _____
Department of MECHANICAL ENGINEERING
August 21, 1984

Certified by _____
David Gordon Wilson
Thesis Supervisor

Accepted by _____
Warren M. Rohsenow, Chairman
Departmental Committee on Graduate Studies

APPLICATION OF ANALYTICAL CENTRIFUGAL-PUMP PERFORMANCE MODELS IN TWO-PHASE FLOW

by

JAMES EDWARD KORENCHAN

Submitted to the Department of MECHANICAL ENGINEERING on August 21, 1984 in partial fulfillment of the requirements for the degree of MASTER OF SCIENCE.

Abstract

An analytical/semi-empirical model developed at MIT to correlate centrifugal-pump performance in two-phase flow was applied to experimental steam/water data produced by Combustion Engineering, Inc. on a 1/5-scale nuclear-reactor pump system. Performance parameters (head and flow coefficients, head-loss and head ratios, void fractions, and system pressures) were correlated and plotted for data in the first, second, and third flow quadrants. Results confirmed the dependence of two-phase pump performance on flow coefficient, void fraction, and system pressure. Experience was gained in the application of the MIT model to a new set of data.

The head-loss-ratio correlation was found to be effective for the first quadrant, but application in the second and third quadrants was not successful because of questionable formulation of the reverse-flow theoretical performance. Correlation by head-ratio was deemed to be more appropriate for the second and third quadrants.

Pump head degradation was found to decrease with increasing flow coefficient, and qualitative results generally agreed with those of other works. Correlation by system pressure and the distinction between upstream and pump-average parameters were stressed in this analysis.

Thesis Supervisor: David Gordon Wilson
Title: Professor of Mechanical Engineering

ACKNOWLEDGEMENTS

I am deeply grateful to Professor David Gordon Wilson, whose expertise, advice, support, and personality enabled me to undertake and complete this research with professional exhilaration and fulfillment.

I affectionately appreciate the continued support of the members of my family, especially my parents, whose faith and love have been inspirational in all of my endeavors.

I am also grateful to my friends, both old and new, who have enriched my educational and social experience at MIT.

Finally, I wish to thank the General Motors Corporation, my employer, for sponsoring these graduate studies at MIT through the GM Fellowship Program.

TABLE OF CONTENTS

LIST OF FIGURES

LIST OF SYMBOLS

Nomenclature

A	flow area
a	two-phase property function $\equiv \frac{\alpha}{1 - \alpha} \frac{\rho_V}{\rho_L}$
b	blade width
C	absolute fluid velocity
d	diameter
f_{tp}	two-phase flow function
g	gravitational acceleration = 9.81 m/s^2 = 32.2 ft/s^2
g_c	gravitational constant = 1.00 (kg m)/(N s^2) = 32.2 (lbm ft)/(lbf s^2)
H	head
H^*	head-loss ratio $\equiv \frac{\Delta H_{o,tp,th} - \Delta H_{o,tp}}{\Delta H_{o,sp,th} - \Delta H_{o,sp}}$
h	enthalpy
K	geometric constant
$\dot{m}$	mass flow per unit time
N	pump impeller speed, rpm
N_s	pump specific speed, $(rpm)(gpm)^{0.5}/(ft)^{0.75}$
p	fluid pressure
Q	volumetric flow per unit time
r	radius
s	slip-velocity ratio
t	impeller blade thickness
u	impeller peripheral velocity
V	fluid velocity
W	fluid velocity relative to impeller
$\dot{W}$	work done by impeller per unit time
x	flow quality $\equiv m_V/m_T$
z	number of impeller blades
z	elevation
α	area void fraction $\equiv A_V/A_T$
α	angle of fluid velocity C relative to meridional direction
β	angle of fluid velocity W relative to tangential direction
β'	impeller blade angle relative to tangential direction

γ	angle of fluid velocity W relative to meridional direction
Δ	property or parameter change
δ	flow deviation angle $\equiv \beta' - \beta$
μ	impeller flow slip factor $\equiv C_{\theta 2}/C_{\theta 2,th}$
ρ	fluid density
ϕ	flow coefficient $\equiv C_m/u$
ψ	work coefficient $\equiv g_c \Delta h_o/u_2^2$
ψ'	head coefficient $\equiv g\Delta H_o/u_2^2$
ω	pump impeller angular speed, rad/s

Subscripts

o	total, static plus dynamic, stagnation value
1	flow plane at (normal) entrance to impeller
1h	hub (inner) intersection of this plane
1s	shroud (outer) intersection of this plane
2	flow plane at (normal) exit of impeller
2i	inner-shroud intersection of this plane
2o	outer-shroud intersection of this plane
3	flow plane at (normal) entrance to diffuser
avg	arithmetic average
be	best-efficiency point, design point
L	liquid
m	meridional, normal to peripheral
m	mean effective
rated	rated conditions
sp	single-phase
T	total, liquid plus vapor
th	theoretical
tp	two-phase
ups	upstream
V	vapor
θ	tangential

1. INTRODUCTION

1.1. Background

The United States nuclear industry employs centrifugal pumps in the primary coolant circuits of the majority of pressurized water reactors (PWRs). These pumps circulate light water under subcooled, pressurized conditions through the core and steam generators. One possible failure mode affecting the ability to cool the core is the loss-of-coolant accident (LOCA). A LOCA is envisioned as a full or partial rupture of the piping at any point in the closed-loop system. During the transient period immediately following a rupture, a blowdown process occurs which reduces the loop pressure (of the order of 14000 kPa or 2000 psi) to near atmospheric pressure. The duration of this depressurization transient depends on the extent of the rupture. Pressurized water flashes into steam through the loop, producing two-phase flow conditions. The performance of the pump(s) in two-phase flow is problematic and is the subject of current research.

The pressure difference between the coolant water and the atmosphere is many times larger than the normal operating pressure rise through the pump (of the order of 700 kPa or 100 psi). Therefore, water will flow toward the rupture regardless of its location relative to the pump, at least in the early part of the transient depressurization. If the pipe break were to occur near the discharge side of the pump, the resulting flow could be well above the pump operating range (i.e., forced flow). In general, any combination of forward (normal) flow through the pump and forward (normal) impeller rotation is known as first-quadrant operation. A break occurring on the suction leg of the pump would likely cause reverse flow through the pump. The conjunction of reverse pump flow and forward rotation is called second-quadrant operation. Surmising further, the turbining action of reversed flow might reverse the impeller rotation, if there is no mechanical anti-reverse device; such a condition is called third-quadrant operation. Fourth-quadrant operation (forward flow and reversed

rotation) is inconceivable from a practical point of view.

The behavior of the centrifugal pump under two-phase flow conditions must be understood and predictable in order to justify a given course of action in the event of a LOCA. Consequently, research effort has been directed toward the modeling of the two-phase pump characteristics; the desired result is the application of reliable models in the nuclear industry.

1.2. Previous Work

Prior to 1977, there were several empirical models for two-phase pump behavior. Each model made use of some form of a head-degradation factor which related two-phase performance characteristics to single-phase characteristics at given flow conditions. These models differed primarily in the form of the factor and in the parameters used to correlate the empirical data. In general, the applicability of each model as a predictive tool was limited to the particular pump system and flow arrangement from which the experimental data were generated. A review of these models was conducted by Wilson, et al. [1977].

A semi-empirical method developed by J. Mikielewicz and D. G. Wilson at MIT (Wilson, et al. [1979]) defined a head-loss ratio as the ratio of the pump head losses in two-phase flow to the head losses in single-phase flow at the same flow coefficient. Subsequent testing on a low-pressure, air/water pump facility at MIT yielded acceptable model correlation. Head-loss ratio was found to be a function of void fraction and flow coefficient (flow regime, in general), and the model exhibited adequate predictive capabilities. Furthermore, the model provided analytical justification for applying the results of one pump system to other pump systems.

In response to a lack of a sufficient data base, the Electric Power Research Institute (EPRI) contracted Combustion Engineering, Inc. (C-E) of Windsor, Connecticut to generate a library of single- and two-phase pump performance data. The C-E test pump and its local

piping were constructed to a 1/5 geometric scale of the Palisades nuclear reactor system. Both steady-state and transient data were collected in flow conditions, temperatures, and pressures anticipated during a LOCA. The final report was published through EPRI (Kennedy, et al. [1980]).

1.3. Purpose

The intent of this current research was to apply the overall MIT analytical model to the C-E two-phase pump data and to examine the effectiveness of the model by data correlation and comparison with earlier results. Expected model weaknesses in the treatment of the variation of two-phase flow parameters through the pump and system pressure effects were given special attention.

The ultimate object of this investigation is to evaluate the MIT model through intensive application of data from an outside source (namely, Combustion Engineering). The discovered strengths and weaknesses of the model will help to define the limits of its applicability as a predictive tool.

2. MIT ANALYTICAL MODELS

The MIT semi-empirical analytical method focuses on the calculation of the head-loss ratio which relates experimental head characteristics with ideal single- and two-phase performance. This section describes the development of the ideal, theoretical performance relations and the application of the head-loss-ratio method in each of the first three quadrants. The presentation follows that given by Chan [1977] and Wilson, et al. [1979].

2.1. Theoretical-Performance Derivations

Along any given streamline through the pump, the Euler equation relates the change of enthalpy of, or work done by, the fluid to the change in angular momentum of the fluid into and out of the impeller.

$$\frac{\dot{W}}{\dot{m}} = g_c \Delta h_o \equiv g_c(h_{o2} - h_{o1}) = u_2 C_{\theta 2} - u_1 C_{\theta 1} \tag{2-1}$$

Equation (2-1) is of general validity for single- or two-phase flow assuming steady and adiabatic conditions.

The general one-dimensional, single-phase-flow velocity triangles for the impeller inlet and outlet are shown in Figure (2-1). The relative flow angle at impeller outlet, β_2, is equal to the blade angle, β_2', less the angle of deviation, δ, due to slip.

$$\beta_2 = \beta_2' - \delta$$

$$\tan \beta_2 = \frac{C_{m2}}{u_2 - C_{\theta 2}}$$

$$\frac{C_{\theta 2}}{u_2} = 1 - \frac{C_{m2}}{u_2 \tan \beta_2}$$

The absolute flow angle at impeller inlet, α_1, is measured relative to the axial direction for

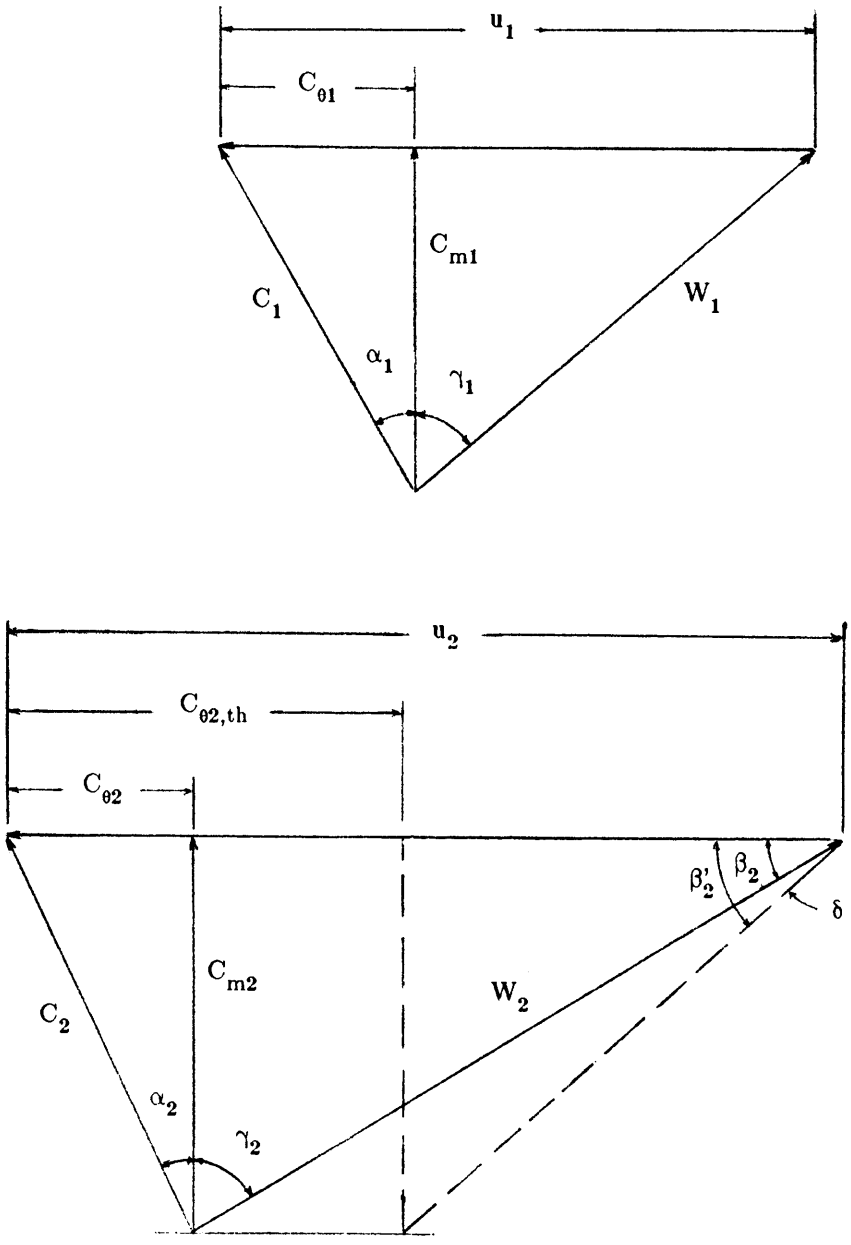

FIGURE 2-1: VELOCITY TRIANGLES AT IMPELLER INLET AND OUTLET

axial-entry pumps with higher specific speeds.

$$\tan \alpha_1 = \frac{C_{\theta 1}}{C_{m1}}$$

$$\frac{C_{\theta 1}}{u_1} = \frac{C_{m1} \tan \alpha_1}{u_1} = 1 - \frac{C_{m1} \tan \gamma_1}{u_1}$$

Letting the flow coefficient, ϕ, be defined as

$$\phi \equiv \frac{C_m}{u}$$

and the work coefficient, ψ, be defined as

$$\psi \equiv \frac{g_c \Delta h_o}{u_2^2}$$

the Euler equation for a centrifugal pump in single-phase flow becomes

$$\psi = 1 - \frac{C_{m2}}{u_2 \tan \beta_2} - \frac{u_1^2 - u_1 C_{m1} \tan \gamma_1}{u_2^2}$$

$$\psi = 1 - \frac{\phi_2}{\tan \beta_2} - \left(\frac{d_1}{d_2}\right)^2 (1 - \phi_1 \tan \gamma_1) \qquad (2\text{-}2)$$

We choose to model two-phase flow as two separate mass flows, liquid and vapor, with presumably different values of velocity, C_θ and C_m, at the impeller inlet and outlet. Euler's equation becomes

$$\psi_{tp} = (1 - x_2) \frac{C_{\theta L2}}{u_2} + x_2 \frac{C_{\theta V2}}{u_2}$$

$$- \left(\frac{d_1}{d_2}\right)^2 \left((1 - x_1) \frac{C_{\theta L1}}{u_1} + x_1 \frac{C_{\theta V1}}{u_1} \right)$$

By assuming that both the liquid and vapor streams leave the impeller in the same direction

(relative angle β_2), we can derive from the velocity triangles, as before,

$$\psi_{tp} = (1 - x_2)\left(1 - \frac{C_{mL2}}{u_2 \tan \beta_2}\right) + x_2\left(1 - \frac{C_{mV2}}{u_2 \tan \beta_2}\right)$$

$$- \left(\frac{d_1}{d_2}\right)^2 \left[(1 - x_1)\left(1 - \frac{C_{mL1} \tan \gamma_1}{u_1}\right) + x_1\left(1 - \frac{C_{mV1} \tan \gamma_1}{u_1}\right)\right] \qquad (2\text{-}3)$$

From continuity and the definition of void fraction, α, we have at the outlet

$$C_{mL2} = \frac{\dot{m}_{L2}}{\rho_{L2} A_{L2}} = \frac{\dot{m}_T (1 - x_2)}{\rho_{L2}(1 - \alpha_2) A_{T2}}$$

$$C_{mV2} = \frac{\dot{m}_{V2}}{\rho_{V2} A_{V2}} = \frac{\dot{m}_T x_2}{\rho_{V2} \alpha_2 A_{T2}}$$

and similarly for the impeller inlet. Here A_T is the normal flow area at inlet or outlet. We can define a two-phase flow coefficient

$$\phi_{tp} \equiv \frac{\dot{m}_T}{\rho_{tp} A_T u}$$

where the two-phase density is related to void fraction the same as specific volume is related to flow quality

$$\rho_{tp} = (1 - \alpha)\rho_L + \alpha \rho_V$$

Substituting into equation (2-3), we obtain

$$\psi_{tp} = \left[1 - \frac{\phi_{tp2}}{\tan \beta_2}\left(1 + \frac{\alpha_2}{1 - \alpha_2}\frac{\rho_{V2}}{\rho_{L2}}\right)\left((1 - x_2)^2 + \frac{1 - \alpha_2}{\alpha_2}\frac{\rho_{L2}}{\rho_{V2}} x_2^2\right)\right]$$

$$- \left(\frac{d_1}{d_2}\right)^2 \left[1 - \phi_{tp1} \tan \gamma_1 \left(1 + \frac{\alpha_1}{1 - \alpha_1}\frac{\rho_{V1}}{\rho_{L1}}\right)\left((1 - x_1)^2 + \frac{1 - \alpha_1}{\alpha_1}\frac{\rho_{L1}}{\rho_{V1}} x_1^2\right)\right] \qquad (2\text{-}4)$$

Equation (2-4) can be simplified by defining a two-phase property function

$$a \equiv \frac{\alpha}{1 - \alpha} \frac{\rho_V}{\rho_L}$$

and a slip velocity ratio between the two phases

$$s \equiv \frac{C_V}{C_L}$$

By continuity and the above definitions, we can derive

$$x = \frac{as}{1 + as}$$

Making these substitutions, the Euler equation for two-phase flow in a centrifugal pump becomes

$$\psi_{tp} = 1 - \frac{f_{tp2}\phi_{tp2}}{\tan \beta_2} - \left(\frac{d_1}{d_2}\right)^2 (1 - f_{tp1}\phi_{tp1}\tan \gamma_1) \qquad (2\text{-}5)$$

where we have defined a two-phase flow function

$$f_{tp} \equiv \frac{(1 + a)(1 + as^2)}{(1 + as)^2}$$

In a single-phase flow, we have $\alpha = a = 0$ and, thus, $f_{tp} = 1.0$; consequently, equation (2-5) becomes identical to the single-phase form, equation (2-2). In homogeneous two-phase flow, $s = 1.0$ (i.e., no slip), and again the two-phase flow function, f_{tp}, is unity (yielding equation (2-2) for the theoretical two-phase head).

2.2. Head-Loss-Ratio Method

2.2.1. General description

The change in enthalpy through the pump is most effectively determined by measuring the change in total head across the pump. The total head is defined as

$$\Delta H_o \equiv \frac{p_2 - p_1}{\rho g/g_c} + \frac{V_2^2 - V_1^2}{2g} + (z_2 - z_1) \tag{2-6}$$

and represents the change in fluid energy by virtue of its pressure and elevation (static-head change) and its velocity (dynamic-head change). For adiabatic, inviscid flow it can be shown that the change in total head is directly proportional to the change in enthalpy through the pump; in fact, we find that $g\Delta H_o = g_c \Delta h_o$. We define a head coefficient as

$$\psi' \equiv \frac{g\Delta H_o}{u_2^2} = \frac{g_c \Delta h_o}{u_2^2} \equiv \psi \tag{2-7}$$

and note that the head and work coefficients are identical under the stated conditions. The head-loss ratio, H^*, is defined as

$$H^* \equiv \frac{\Delta H_{o,tp,th} - \Delta H_{o,tp}}{\Delta H_{o,sp,th} - \Delta H_{o,sp}} = \frac{\psi'_{tp,th} - \psi'_{tp}}{\psi'_{sp,th} - \psi'_{sp}} \tag{2-8}$$

which is the ratio of the two-phase head losses to the single-phase head losses at the same flow coefficient. The theoretical head coefficients are calculated from some form of the ideal Euler equation (2-5).

The head-loss ratio, essentially a function of flow regime, is the key correlating parameter of the MIT performance model. The head losses which the ratio empirically relates are due to flow-separation, wall-friction, and the interaction of individual phases (two-phase

flow only). By normalizing two-phase head *losses* to single-phase *losses*, as opposed to normalizing the two-phase *head* to the single-phase *head* (ψ'_{tp}/ψ'_{sp}), theoretical performance has been introduced along with empirical performance. In this way, it is anticipated that the two-phase performance dependence on a particular pump geometry is diminished.

Plots of head-loss ratio against void fraction for specified flow coefficient ranges form the semi-empirical basis for two-phase performance predictions. From the H^* curves of one pump, the two-phase head coefficient of another pump can be calculated for a given void fraction and flow coefficient (provided the desired flow coefficient is in the range of the former pump's experimental range). The accuracy of this prediction can be properly judged only after a library of head-loss-ratio correlations are produced for pumps of varying specific speeds and geometries.

2.2.2. First-quadrant application

For a centrifugal pump operating in the first quadrant (forward flow, forward rotation), the angular momentum at the impeller inlet is very small compared with that at the outlet. If we assume that there is no inlet "swirl" or prerotation, then the Euler equation (2-1) becomes

$$g_c \Delta h_o = u_2 C_{\theta 2}$$

and the derived two-phase flow equation (2-5) simplifies to

$$\psi'_{tp} = 1 - \frac{f_{tp2}\phi_{tp2}}{\tan \beta_2} \tag{2-9}$$

where the equivalence of the work and head coefficients has been assumed (adiabatic, inviscid flow; equation (2-7)).

The theoretical relation for first-quadrant operation can be further simplified by the fact that the two-phase flow function, f_{tp}, is close to unity for practical (LOCA) conditions. Using

values of two-phase slip, s, based on a correlation by Thom [1964], f_{tp} has been shown (Wilson, et al. [1977]; Chan [1977]) to be generally less than a value of 1.05 for steam-water flows with pressures greater than 500 psi (3400 kPa). Maximum values of $f_{tp} \approx 1.10$ occur near high void fractions (α=0.9). Consequently, we can choose to use

$$\psi'_{tp} \approx 1 - \frac{\phi_{tp2}}{\tan \beta_2} \tag{2-10}$$

as the theoretical two-phase Euler equation for a centrifugal pump operating in the first quadrant with no inlet swirl. This equation (2-10) is similarly valid for single-phase flow.

The remaining difficulty in using equation (2-10) is in knowing the slip factor, μ, necessary to calculate the relative flow angle, β_2. The slip factor is defined as

$$\mu \equiv \frac{C_{\theta 2}}{C_{\theta 2,th}}$$

and its relationship to the outlet flow angle can be obtained from Figure 2-1:

$$\tan \beta_2 = \frac{\phi_2}{1 - \mu + \mu\phi_2 \cot \beta'_2} \tag{2-11}$$

Many methods of calculating μ have been published. Stodola [1927] derived an appromixate relationship for the slip factor at the design operating point:

$$\mu_{be} = 1 - \frac{(\pi/z) \sin \beta'_2}{1 - \phi_{2,be} \cot \beta'_2} \tag{2-12}$$

Although it is unrealistic to assume that the slip factor and deviation angle remain constant over a large flow-coefficient range, the head-loss-ratio correlation will not be adversely affected to a great degree. Indeed, without adequate experimental measurement of the relative flow angle over an extended range of flow coefficients, there is no justification for other than a constant-deviation-angle assumption.

Wilson, et al. [1979] recommend the use of an empirical correlation by Noorbakhsh [1973] for determining the slip factor. This correlation produces a slip factor based on experiments made on five pumps of different geometries over somewhat extended flow-coefficient ranges. By obtaining results from a test pump of similar geometry, one attains some empirical justification in letting the slip factor vary over a given flow range.

2.2.3. Second-quadrant application

In the dissipative second quadrant (reverse flow, forward rotation) the two-phase Euler equation (2-5) cannot be applied directly because the flow angles at impeller inlet and outlet are not easily calculable. Also, the first-quadrant assumption of negligible prerotation is unrealistic for the second quadrant. Instead, Wilson, et al. [1979] use the geometry of the pump diffuser (inlet for reverse flow) and the impeller inlet (outlet for reverse flow) to derive the fluid angular momenta for use in the Euler equation (2-1). The critical assumptions are

- the relative outlet flow angle from the impeller in the second quadrant is equal to the relative inlet flow angle for the first quadrant, γ_1, measured from a plane through the axis and at the best-efficiency point; and
- the axial velocity, C_{m1}, is radially uniform.

The final result, which does not make a distinction for two-phase flow (i.e., $f_{tp} = 1.0$) is

$$\psi' = K\left(\frac{r_{1h}}{r_{1s}}\right)^2 \left(1 - \frac{\omega_{be}}{\omega}\frac{Q}{Q_{be}}\right) - \frac{Q \tan \alpha_3}{2\pi b_3 r_2^2 \omega} \tag{2-13}$$

where we have a geometric factor,

$$K = \frac{1}{3}\left(1 + \frac{r_{1h}}{r_{1s}} + \left(\frac{r_{1h}}{r_{1s}}\right)^2\right)$$

and we note that the volumetric flow rate, Q, is negative in the second quadrant and that the angular speed, ω, is positive.

2.2.4. Third-quadrant application

We make the same assumptions in the third quadrant (reverse flow, reverse rotation) that were made in the second. A similar derivation yields

$$\psi' = \frac{Q \tan \alpha_3}{2\pi b_3 r_2^2 \omega} - K\left(\frac{r_{1h}}{r_{1s}}\right)^2 \left(1 - \frac{\omega_{be}}{\omega}\frac{Q}{Q_{be}}\right) \tag{2-14}$$

where K is the same geometric factor as before and we note that both Q and ω are negative in the third quadrant.

3. APPLICATION TO C-E DATA

3.1. C-E Project Background

The jointly-funded Combustion Engineering and Electric Power Research Institute project, entitled Pump Two-Phase Performance Program, came into existence as the result of a U. S. Atomic Energy Commision (AEC) request in 1973. The AEC sought programs for obtaining experimental information which would enable the development of more refined analytical modeling of pump performance under hypothetical LOCA conditions. The objective of the C-E/EPRI project was, therefore, to obtain sufficient steady-state and transient, single- and two-phase empirical data to substantiate present and ultimately improved mathematical models used for LOCA analysis. A full description of the project details and results appears in the C-E final report (Kennedy, et al. [1980]).

3.2. C-E Project Description

As stated earlier, the C-E project used a 1/5-scale model of the Palisades Nuclear Power Plant reactor coolant pumps (see Appendix A for pertinent dimensions and rated performance conditions). In addition, the suction and discharge piping adjacent to the pumps was modeled to the same scale; however, the pump axis was positioned horizontally instead of vertically as in the reactor system. In steady-state testing, steam from a pressure boiler would be mixed with pressurized water at saturated conditions and directed through the test pump in either the forward or reverse direction, depending on the arrangement of the reversible piping. Transient tests to simulate the pressure degradation and two-phase phenomena of a blowdown following a rupture were made by establishing specified steady-state conditions and utilizing a rupture diaphragm.

The basic elements of the test system with the locations and types of accompanying instrumentation are shown in Figure 3-1. The instrumentation included temperature sensors,

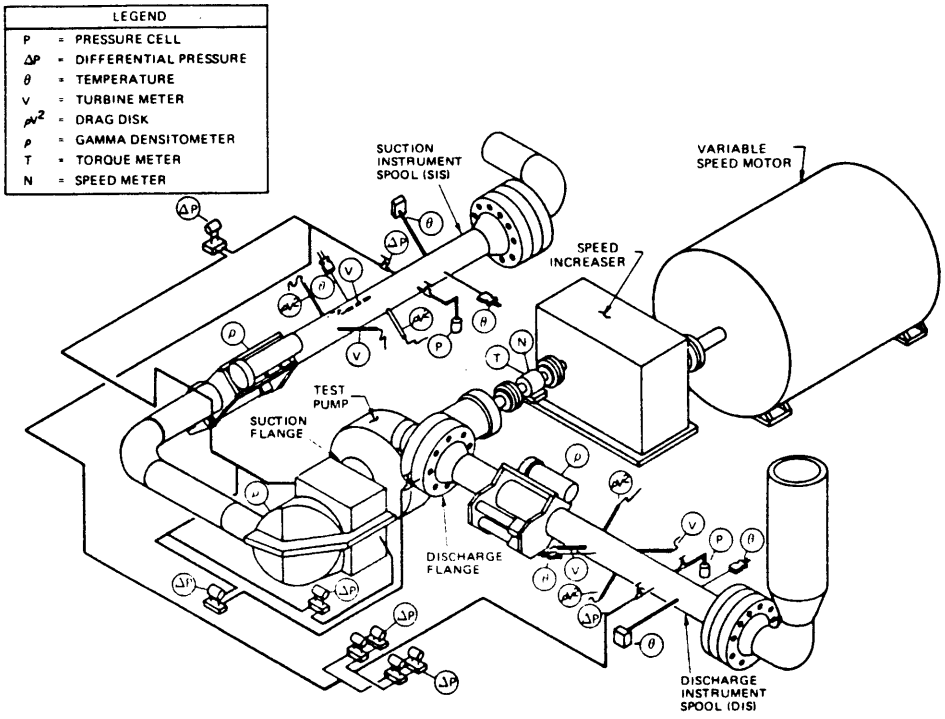

FIGURE 3-1: COMBUSTION ENGINEERING TEST SECTION SCHEMATIC

pressure tranducers, gamma densitometers, drag discs, turbine meters, and flow orifices. Parameters either directly measured or derived from other measurements include pump suction and discharge pressures, temperatures, densities, velocities, volumetric flow rates, and void fractions. In addition, pump speed, shaft torque, and the mass flow rate of the individual steam and water flows entering the system were recorded. Data acquisition systems scanned the instrumentaion, recording time-averaged results and measurement drift.

Most of the test program was devoted to forward pump flow and forward impeller rotation (first quadrant). Much less emphasis was placed on the reverse-flow quadrants because reactor pumps are fitted with anti-reverse-rotation devices and a reverse flow transient would not last long before the pump impeller slowed to a halt. Fourth-quadrant combinations of forward flow and reverse rotation were omitted from the program. For each quadrant of operation tested, a comparable number of single-phase steady-state test runs and two-phase test runs were performed.

3.3. Correlation Parameters

In single-phase pump flow, the performance is correlated by parameters which are derived from the basic measurements of volumetric flow rate, pump head, pump speed, and fluid density. For two-phase flow, void fraction and system pressure are also necessary to define the performance. The head-loss-ratio correlation method requires the calculation of two key parameters: the flow coefficient and the head coefficient. The flow coefficient used here will be defined with respect to the impeller *exit*, regardless of the flow quadrant involved. Consequently, we have (dropping the subscript 2 on ϕ)

$$\phi = \frac{C_{m2}}{u_2}$$

where

$$C_{m2} = \frac{Q}{A_2}$$

and

$$u_2 = \frac{2\pi r_{2,m} N}{60}$$

The net flow area at impeller exit, A_2, is calculated in Appendix A . The head coefficient, ψ' is calculated using equation (2-7) where the total head, ΔH_o, is given by equation (2-6).

Several decisions were made in the present analysis with regards to the selection of the particular measurements used to calculate the correlating parameters; the completeness of the C-E test program afforded various choices. First of all, the static-pressure rise across the pump was taken from suction flange to discharge flange. The C-E data also offered a leg-to-leg Δp; pressure cells were located within the main instrumentation sections several feet ahead of and behind the test pump. Combustion Engineering's own data presentations utilized this leg-to-leg pressure rise (which included the losses in two suction pipe elbows, Figure 3-1) because of the sensor proximity to the other instrumentation (turbine meter, densitometer, etc.) and because of their desire to model the pump *system*, including adjacent piping. The decision here to use the flange-to-flange Δp was made because the analytical model incorporates only the pump (specifically, the impeller) and not any piping losses.

During two-phase flow conditions, significant variations in parameters occur from pump suction to pump discharge; the change in absolute pressure affects the thermodynamic equilibrium between the phases. The variations are most pronounced at low-to-medium void fractions, $0.0 < \alpha < 0.5$. In this analysis, the volumetric flow rates, two-phase densities, and void fractions used were arithmetic averages of the suction and discharge measurements. One reason for this choice is that the fluid averages are more representative of the intra-impeller flow conditions. Also, the use of either the upstream or downstream measurements alone would be less accurate than the use of the averages because of the distance of the

sensors from the test pump. The effect of the parameter variations on the application results is analyzed in Chapter 4.

The void fractions and fluid densities used in this analysis were those computed by Combustion Engineering through the application of an energy balance. Measured mass flow rates of the individual steam and water flows were used to determine the quality and hence the density at mixing based on known saturation densities. Energy corrections for heat gains and losses in the piping legs and for the pump work were made based on temperature, pressure, and flow measurements through the test section. Void-fraction readings (from which density could be calculated) were also obtained through the use of three-beam gamma densitometers, but interpretations of these readings are irresolute because of the non-uniform phase distributions that usually existed in the piping. Furuya [1984] examined the C-E densitometer data and noted that the steam and water flows separated noticeably as they traversed the two 90^{o} elbows ahead of the pump inlet. The variations in the densitometer readings, sometimes as much as 5:1 between beams, preclude their meaningful use.

Calculation of void fraction by the energy balance described above ignores the phenomenon of slip (different relative velocities of steam and water). In fact, the energy-balance void fraction is the volumetric quality of the flow; it is not the actual void fraction, based on cross-sectional area, which would be properly measured by a gamma densitometer. By using the volumetric quality to represent the void fraction, we are assuming that the flow is homogeneous, that is, $s = 1.0$. This assumption does not diminish the value of volumetric quality as a correlating parameter, however. Indeed, Manzano [1980] concluded that the flowing void fraction (volumetric quality) was a better correlating parameter than the actual void fraction, based on results from a low-pressure, air/water test rig at MIT. One justification for the use of the volumetric quality is that the pump impeller blades tend to cut across any non-uniform phase distributions at the pump inlet, creating a more homogeneous mixture.

Since two-phase flows occur at saturated conditions, the system pressure is an indication of the thermodynamic state of the fluid. The average absolute pressure of the fluid within the pump section was included in this analysis as a correlating parameter. The effect of system pressure on two-phase pump performance is analyzed in Chapter 4.

3.4. First-Quadrant Results

The C-E steady-state, first-quadrant flow data appear in Appendix B along with flow and head coefficients for each test point. The least-squares, fourth-degree polynomial fit of the single-phase data (including both water and steam points) was found to be

$$\psi'_{sp} = 0.4692 - 0.05395\phi - 8.334\phi^2 + 14.10\phi^3 - 35.84\phi^4$$

for the flow coefficient range

$$0.00 < \phi < 0.45$$

The root-mean-square error in ψ'_{sp} was 0.0406 for all test points and was 0.0170 for those test points with $\psi'_{sp} > 0$. The single-phase points and curve fit appear in Figures 3-2 and 3-3. Several (13%) of the single-phase points listed in Appendix B were omitted from the curve-fitting process because they deviated significantly from the rest. Most of these anomalies occurred at high flow coefficients ($\phi > 0.25$).

Calculation of the slip factor, μ, at the design operating point by the Stodola equation (2-12) yielded $\mu = 0.57$, while use of the empirical correlation by Noorbakhsh resulted in a roughly constant $\mu \approx 0.58$ over the flow coefficient range $0.07 < \phi < 0.22$. Combining equations (2-10) and (2-11) gives

$$\psi'_{tp,th} \approx \psi'_{sp,th} = \mu\left(1 - \frac{\phi}{\tan \beta'_2}\right)$$

and substitution of the Noorbakhsh slip factor gives

$$\psi'_{tp,th} \approx \psi'_{sp,th} = 0.58 - 0.965\phi$$

which was the theoretical relation used for computing the head-loss ratio H^*.

The system operating pressure most prevalent in the C-E steady-state, two-phase data was 1000 psi (6900 kPa). Consequently, when pressure is not the main correlating parameter, first-quadrant plots contain only test points with pressures near 1000 psi. Plots of the two-phase test points, correlated by void fraction and illustrating their relation to the single-phase and theoretical curves, are given in Figures 3-4 and 3-5.

The head-loss ratios, H^*, and head ratios, $\psi'_{tp}/\ \psi'_{sp}$, for the two-phase test points are given in Appendix C . Listed with each point for correlation purposes are the upstream and average void fractions and the system pressure.

Plots of head-loss ratio and head ratio against void fraction, correlated by either flow coefficient or system pressure, are given in Figures 3-6, 3-7, 3-8, 3-9, 3-10, and 3-11. The curves sketched through the points are understood to be approximate correlating curves.

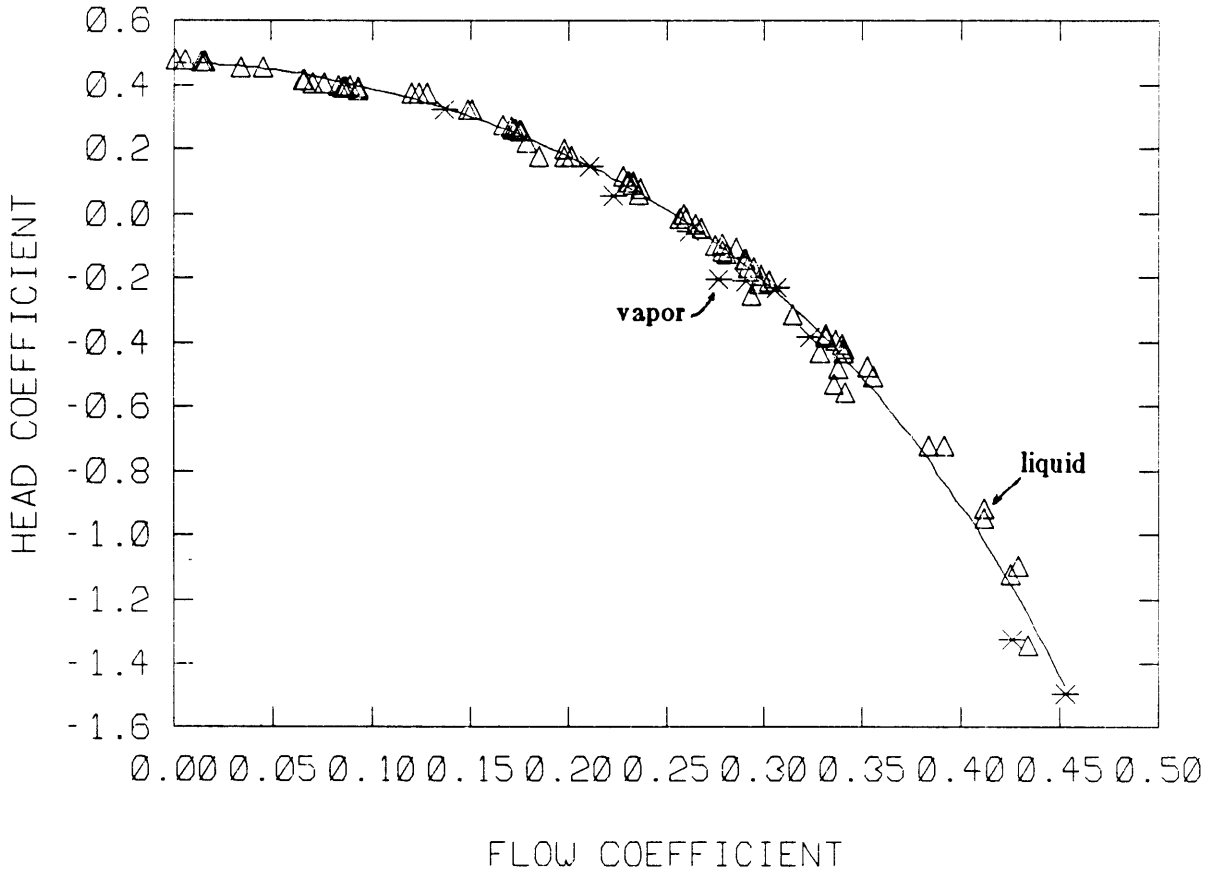

FIGURE 3-2: HEAD COEFFICIENT ψ' VS. FLOW COEFFICIENT ϕ, FIRST QUADRANT, SINGLE PHASE

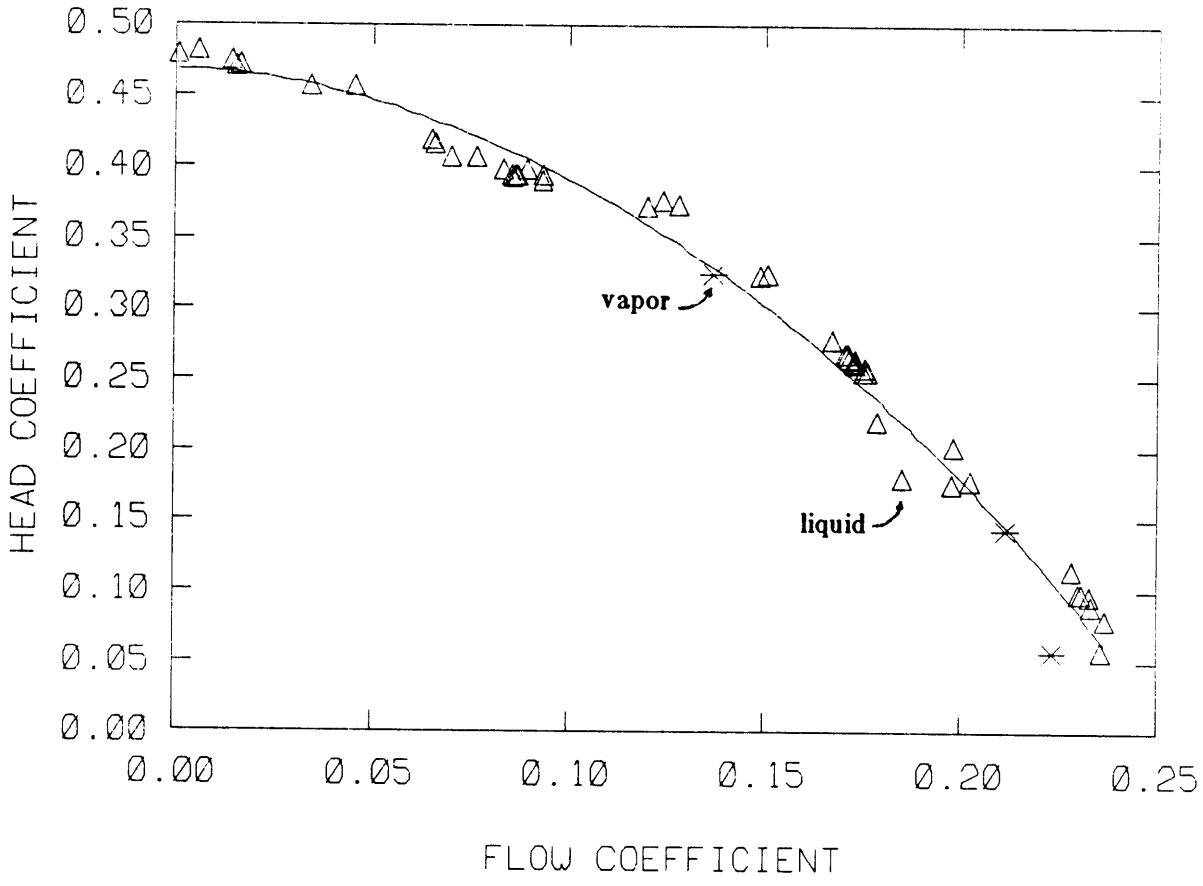

FIGURE 3-3: HEAD COEFFICIENT ψ' VS. FLOW COEFFICIENT ϕ, FIRST QUADRANT, SINGLE PHASE, $0.00 < \phi < 0.25$

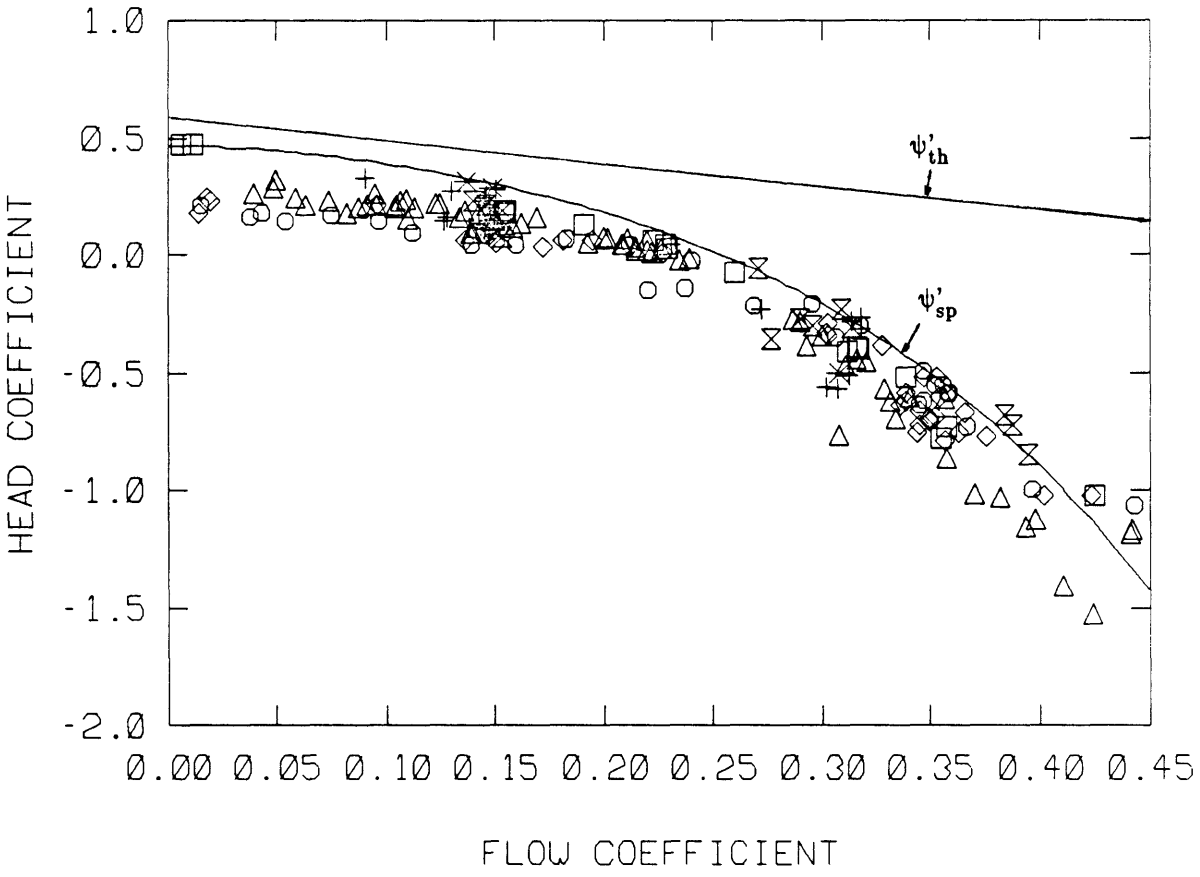

$\ast$ $0.0 < \alpha_{avg} < 0.1$
$+$ $0.1 < \alpha_{avg} < 0.2$
$\square$ $0.2 < \alpha_{avg} < 0.3$
$\triangle$ $0.3 < \alpha_{avg} < 0.5$
$\diamond$ $0.5 < \alpha_{avg} < 0.7$
$\circ$ $0.7 < \alpha_{avg} < 0.9$
$\boxtimes$ $0.9 < \alpha_{avg} < 1.0$

$450 < p < 1050$ psi

FIGURE 3-4: HEAD COEFFICIENT ψ' VS. FLOW COEFFICIENT ϕ, FIRST QUADRANT, TWO PHASE

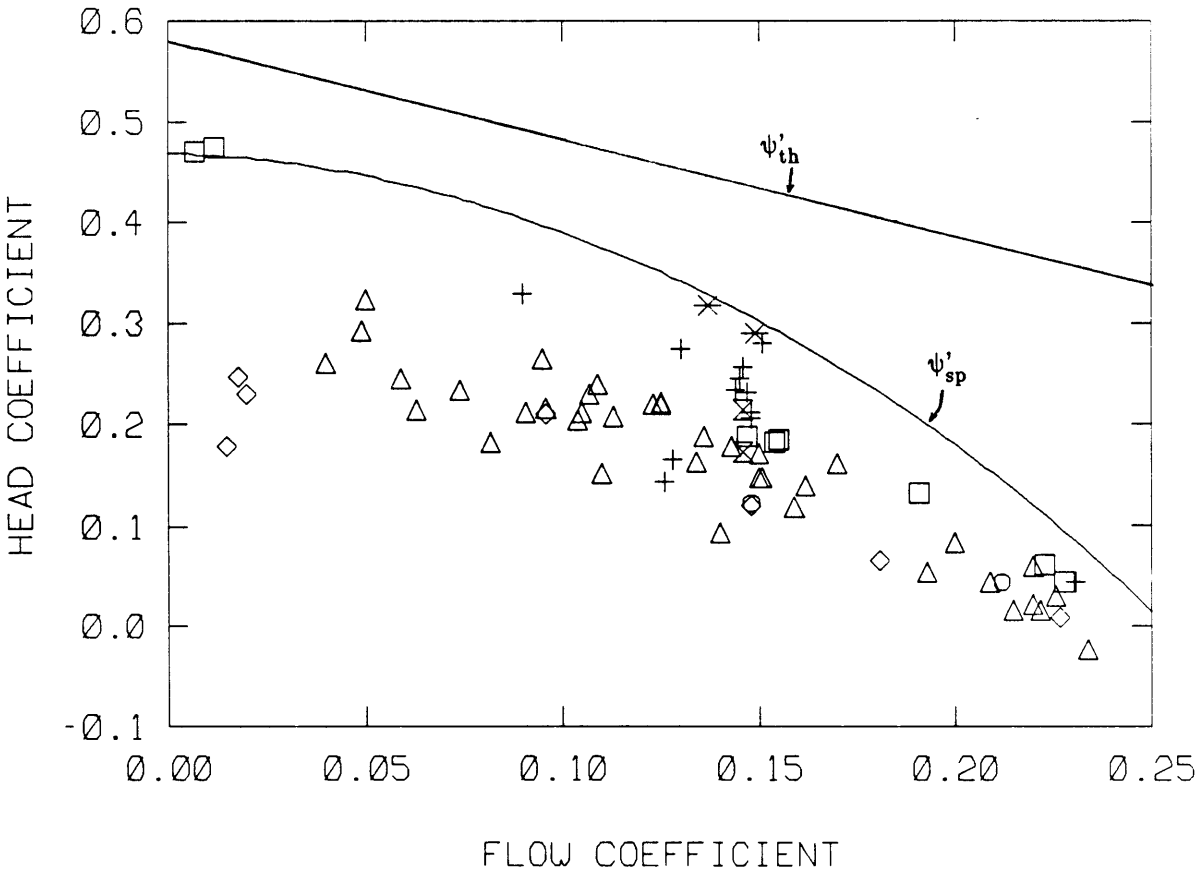

$\ast$ $0.0 < \alpha_{avg} < 0.1$
$+$ $0.1 < \alpha_{avg} < 0.2$
$\square$ $0.2 < \alpha_{avg} < 0.3$
$\triangle$ $0.3 < \alpha_{avg} < 0.5$
$\diamond$ $0.5 < \alpha_{avg} < 0.7$
$\circ$ $0.7 < \alpha_{avg} < 0.9$
$\boxtimes$ $0.9 < \alpha_{avg} < 1.0$

$950 < p < 1050$ psi

FIGURE 3-5: HEAD COEFFICIENT ψ' VS. FLOW COEFFICIENT ϕ, FIRST QUADRANT, TWO PHASE, $0.00 < \phi < 0.25$

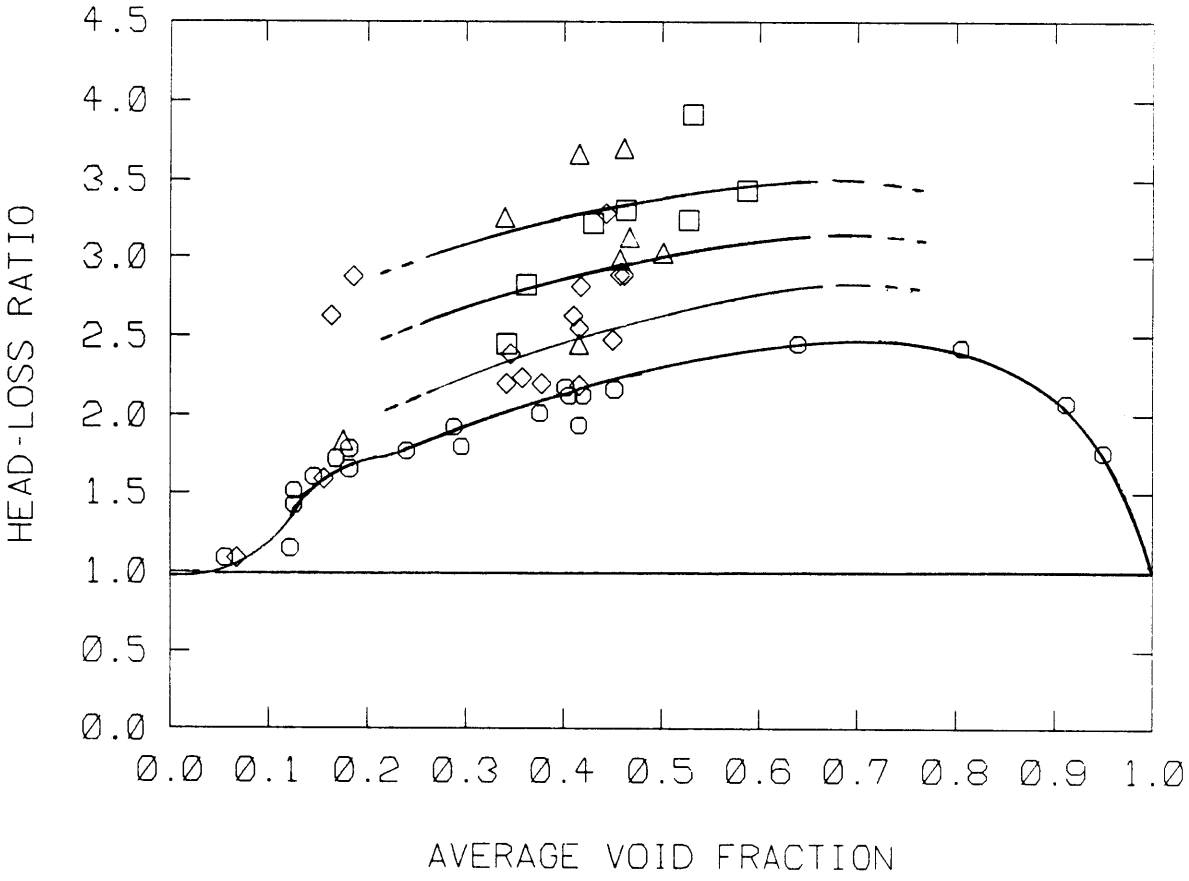

□ $0.01 < \phi < 0.06$
△ $0.06 < \phi < 0.10$
◇ $0.10 < \phi < 0.14$
○ $0.14 < \phi < 0.16$

$950 < p < 1050$ psi

FIGURE 3-6: HEAD-LOSS RATIO H^* VS. AVERAGE VOID FRACTION α_{avg}, FIRST QUADRANT, CORRELATED BY FLOW COEFFICIENT ϕ, $0.01 < \phi < 0.16$

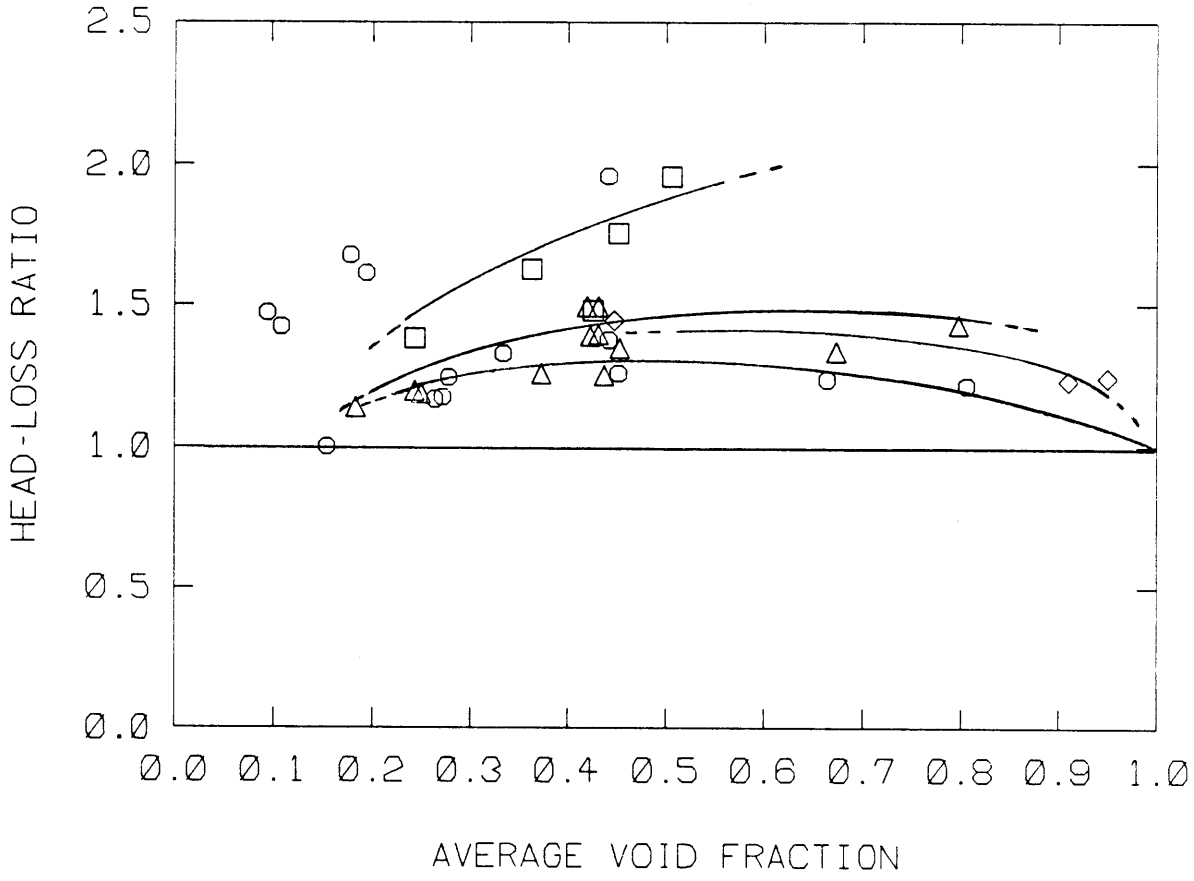

□ $0.16 < \phi < 0.20$
△ $0.20 < \phi < 0.24$
◇ $0.26 < \phi < 0.30$
○ $0.30 < \phi < 0.35$

$950 < p < 1050$ psi

FIGURE 3-7: HEAD-LOSS RATIO H^* VS. AVERAGE VOID FRACTION α_{avg}, FIRST QUADRANT, CORRELATED BY FLOW COEFFICIENT ϕ, $0.16 < \phi < 0.35$

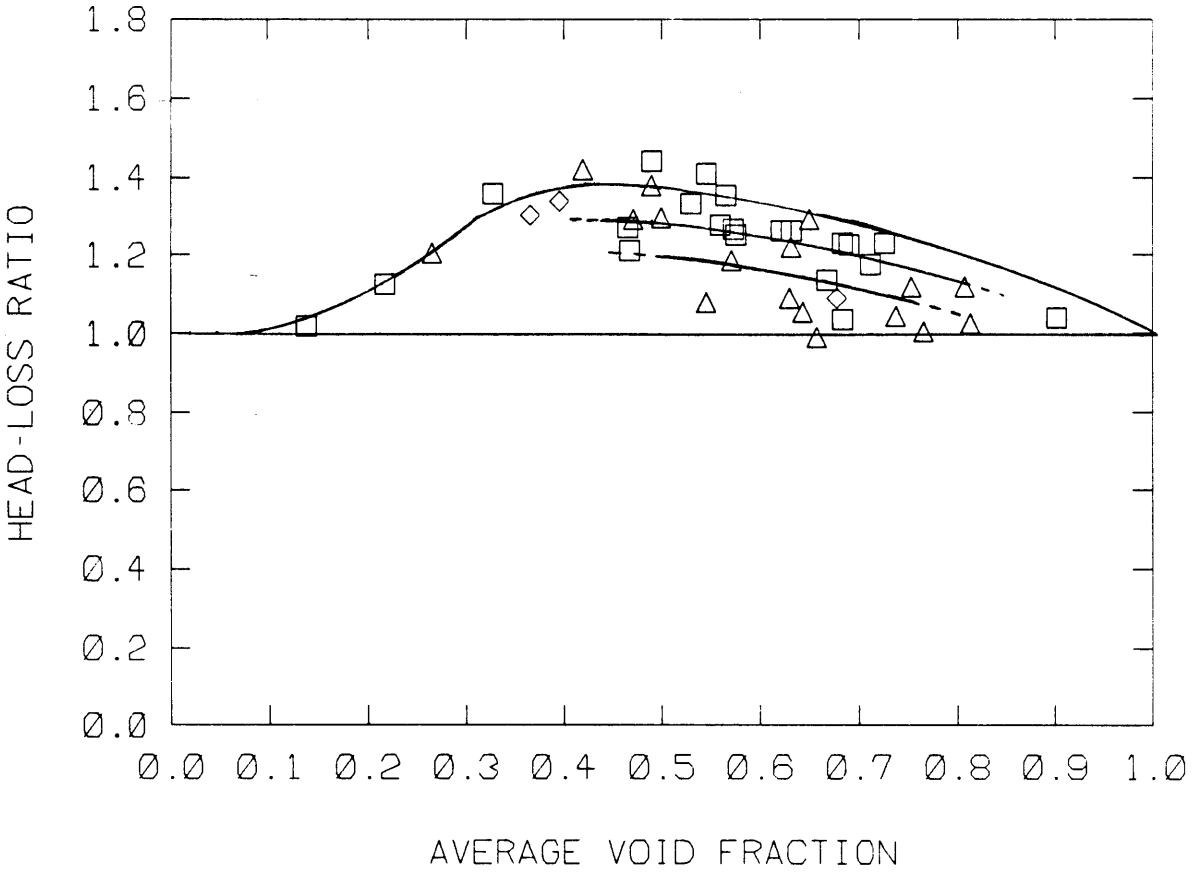

□ $0.30 < \phi < 0.35$
△ $0.35 < \phi < 0.40$
◇ $0.40 < \phi < 0.45$

$600 < p < 950$ psi

FIGURE 3-8: HEAD-LOSS RATIO H^* VS. AVERAGE VOID FRACTION α_{avg}, FIRST QUADRANT, CORRELATED BY FLOW COEFFICIENT ϕ, $0.30 < \phi < 0.45$

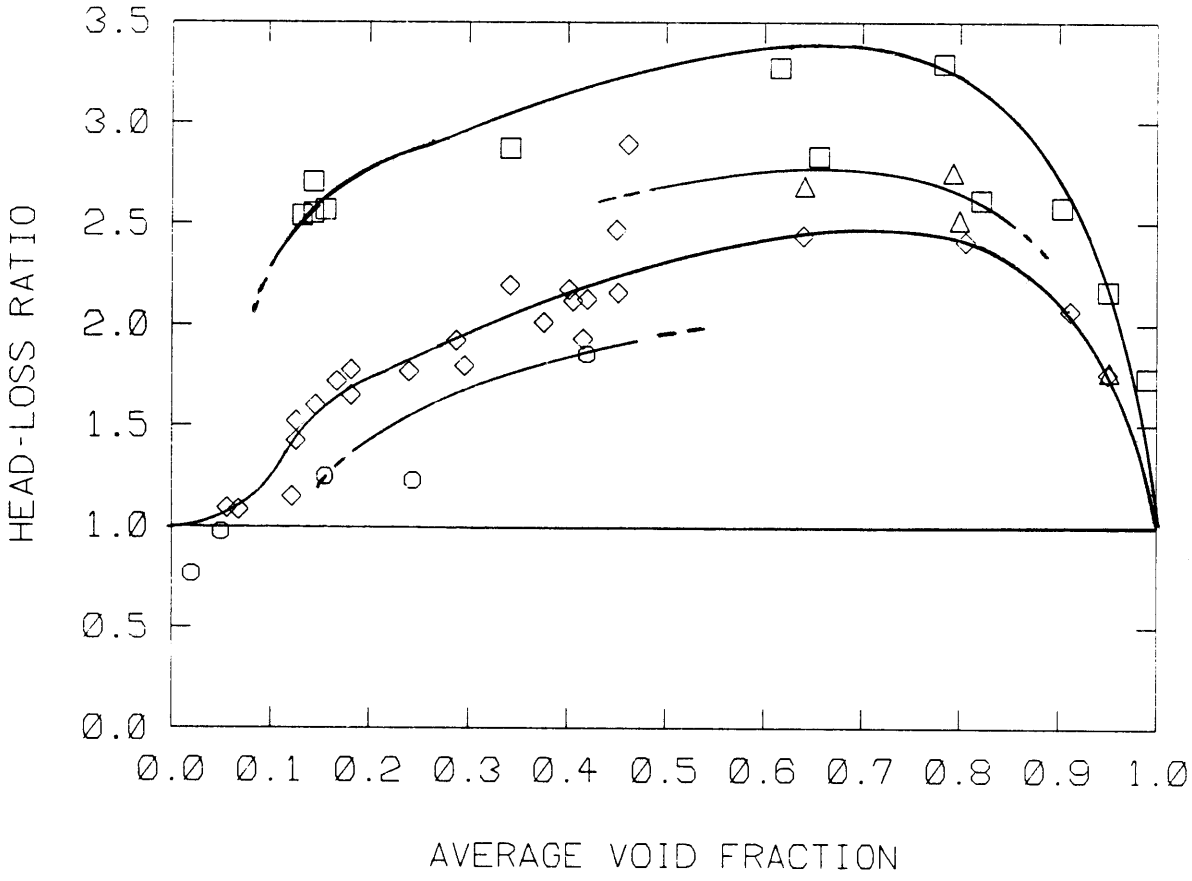

□ 470 < p < 490 psi
△ 840 < p < 860 psi
◇ 950 < p < 1030 psi
○ 1110 < p < 1230 psi

$0.134 < \phi < 0.162$

FIGURE 3-9: HEAD-LOSS RATIO H^* VS. AVERAGE VOID FRACTION α_{avg}, FIRST QUADRANT, CORRELATED BY SYSTEM PRESSURE p

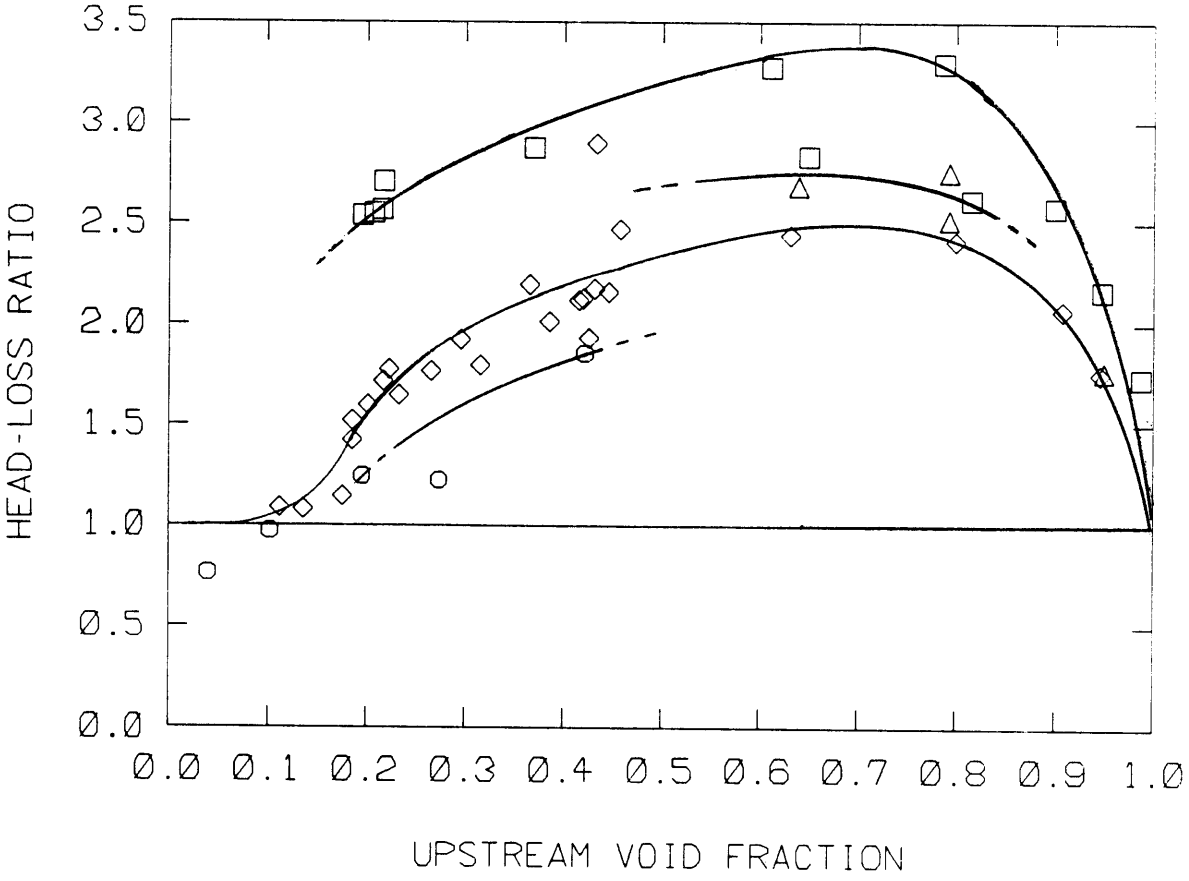

□ 470 < p < 490 psi
△ 840 < p < 860 psi
◇ 950 < p < 1030 psi
○ 1110 < p < 1230 psi

$0.134 < \phi < 0.162$

FIGURE 3-10: HEAD-LOSS RATIO H^* VS. UPSTREAM VOID FRACTION α_{ups}, FIRST QUADRANT, CORRELATED BY SYSTEM PRESSURE p

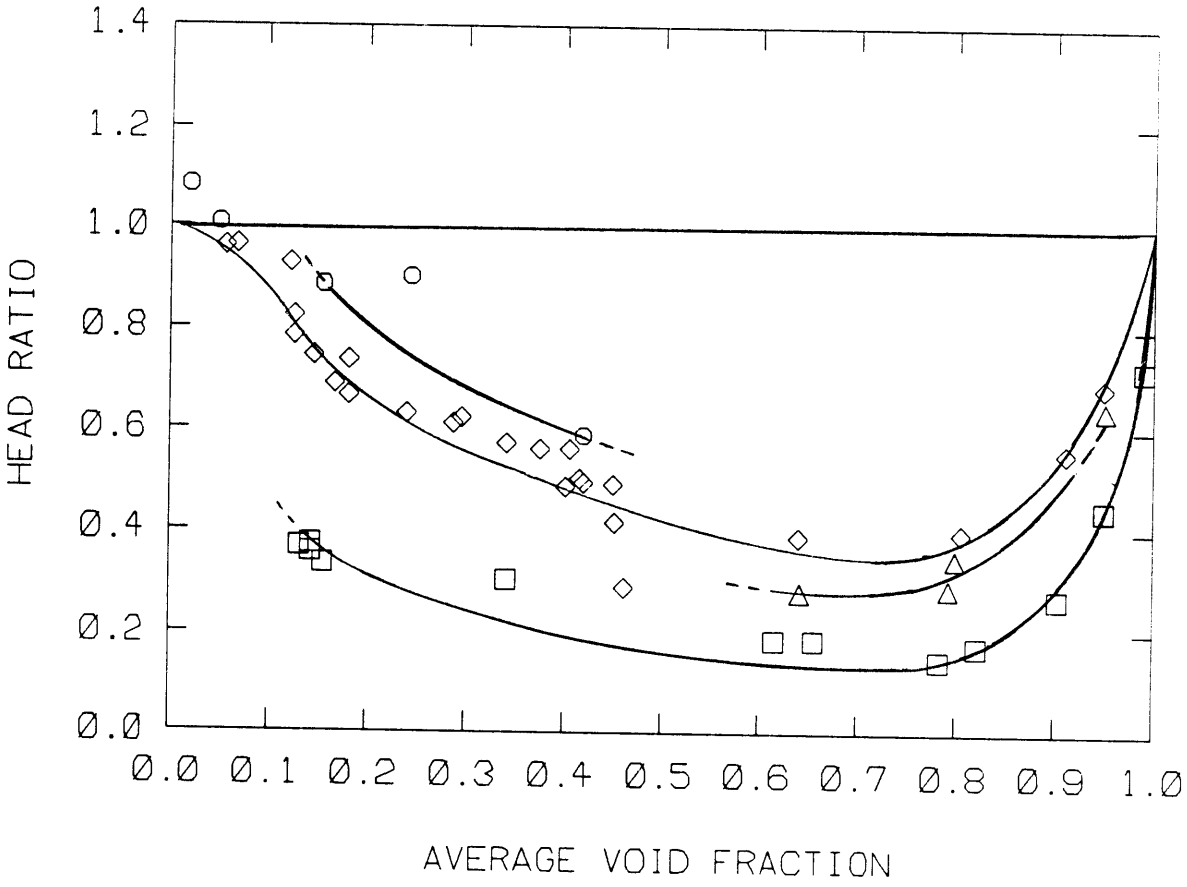

□ 470 < p < 490 psi
△ 840 < p < 860 psi
◇ 950 < p < 1030 psi
○ 1110 < p < 1230 psi

$0.134 < \phi < 0.162$

FIGURE 3-11: HEAD RATIO ψ'_{tp}/ψ'_{sp} VS. AVERAGE VOID FRACTION α_{avg}, FIRST QUADRANT, CORRELATED BY SYSTEM PRESSURE p

3.5. Second-Quadrant Results

The C-E steady-state, second-quadrant flow data appear in Appendix B, and the correlating parameters for two-phase performance are listed in Appendix C . The least-squares polynomial fit used for single-phase performance was

$$\psi'_{sp} = 0.5301 + 1.083\phi + 24.67\phi^2 + 5.049\phi^3 + 1.405\phi^4$$

for the flow coefficient range

$$-0.75 < \phi < 0.00$$

with a root-mean-square error in ψ'_{sp} of 0.0745 . The single-phase plot appears in Figure 3-12.

Theoretical performance for the second quadrant was calculated using equation (2-13). The theoretical-performance line is given in Figure 3-13 along with the second-quadrant, two-phase points and their relation to the single-phase curve.

Because the theoretical-performance line intersects the single-phase curve for the second quadrant, the head-loss ratio correlation is inappropriate. This observation is interpreted in Chapter 4. A plot of head ratio against void fraction for the second quadrant is given in Figure 3-14.

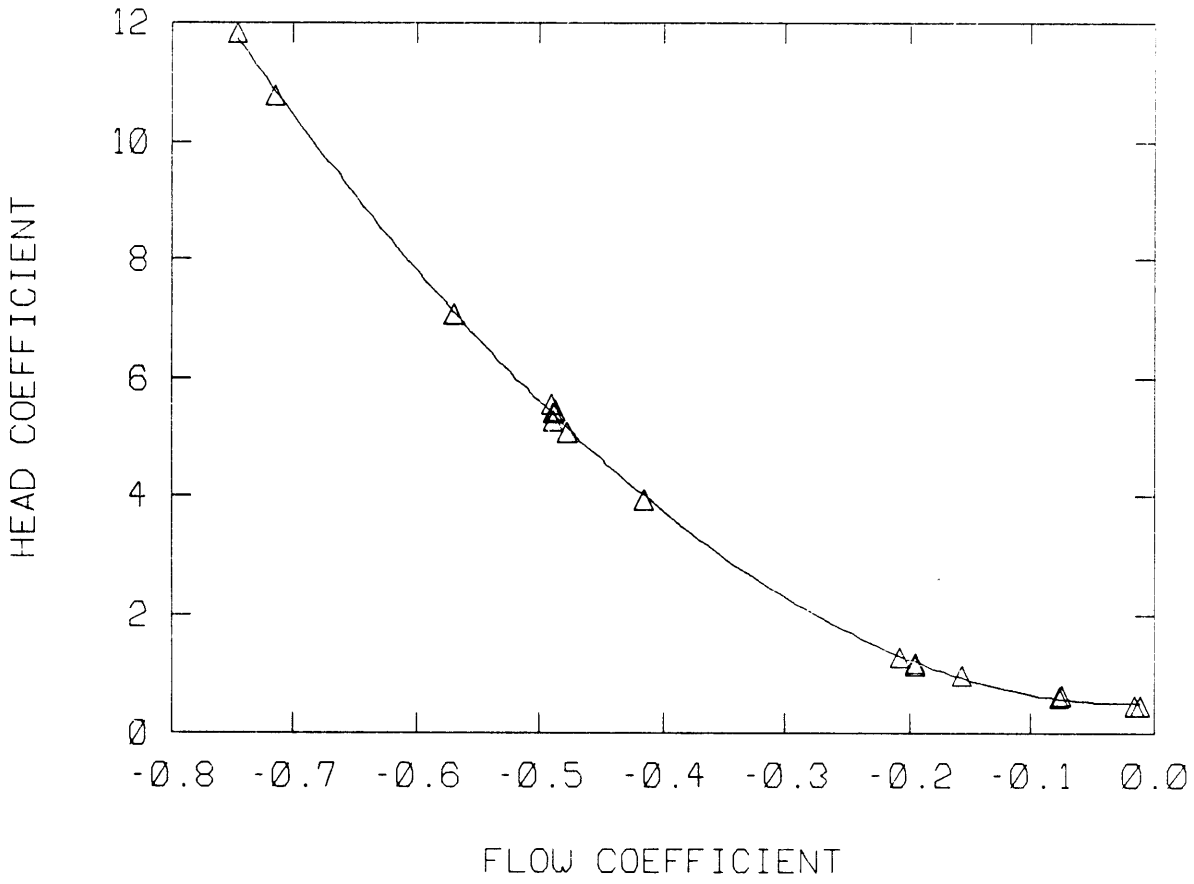

FIGURE 3-12: HEAD COEFFICIENT ψ' VS. FLOW COEFFICIENT ϕ, SECOND QUADRANT, SINGLE PHASE

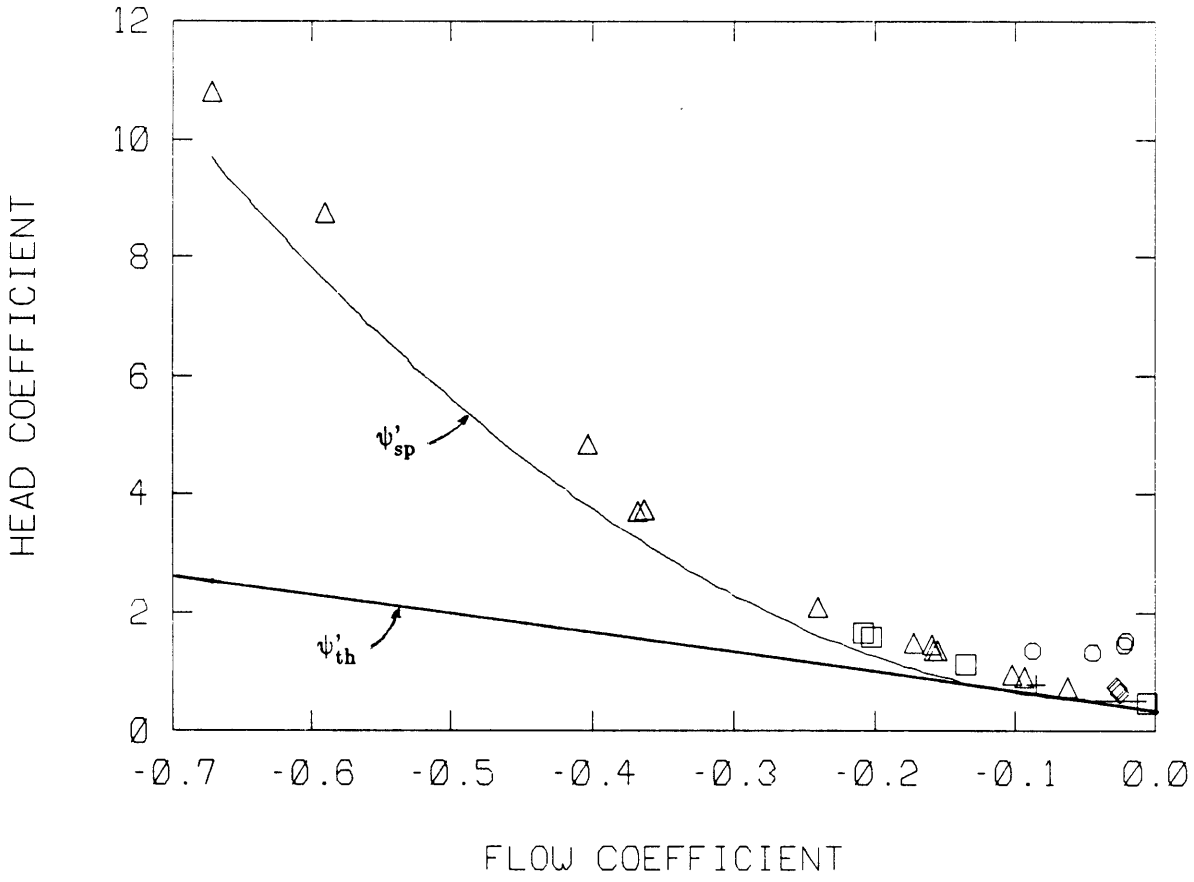

$\ast$ $0.0 < \alpha_{avg} < 0.1$
$+$ $0.1 < \alpha_{avg} < 0.2$
$\square$ $0.2 < \alpha_{avg} < 0.3$
$\triangle$ $0.3 < \alpha_{avg} < 0.5$
$\diamond$ $0.5 < \alpha_{avg} < 0.7$
$\circ$ $0.7 < \alpha_{avg} < 0.9$
$\boxtimes$ $0.9 < \alpha_{avg} < 1.0$

$820 < p < 1160$ psi

FIGURE 3-13: HEAD COEFFICIENT ψ' VS. FLOW COEFFICIENT ϕ, SECOND QUADRANT, TWO PHASE

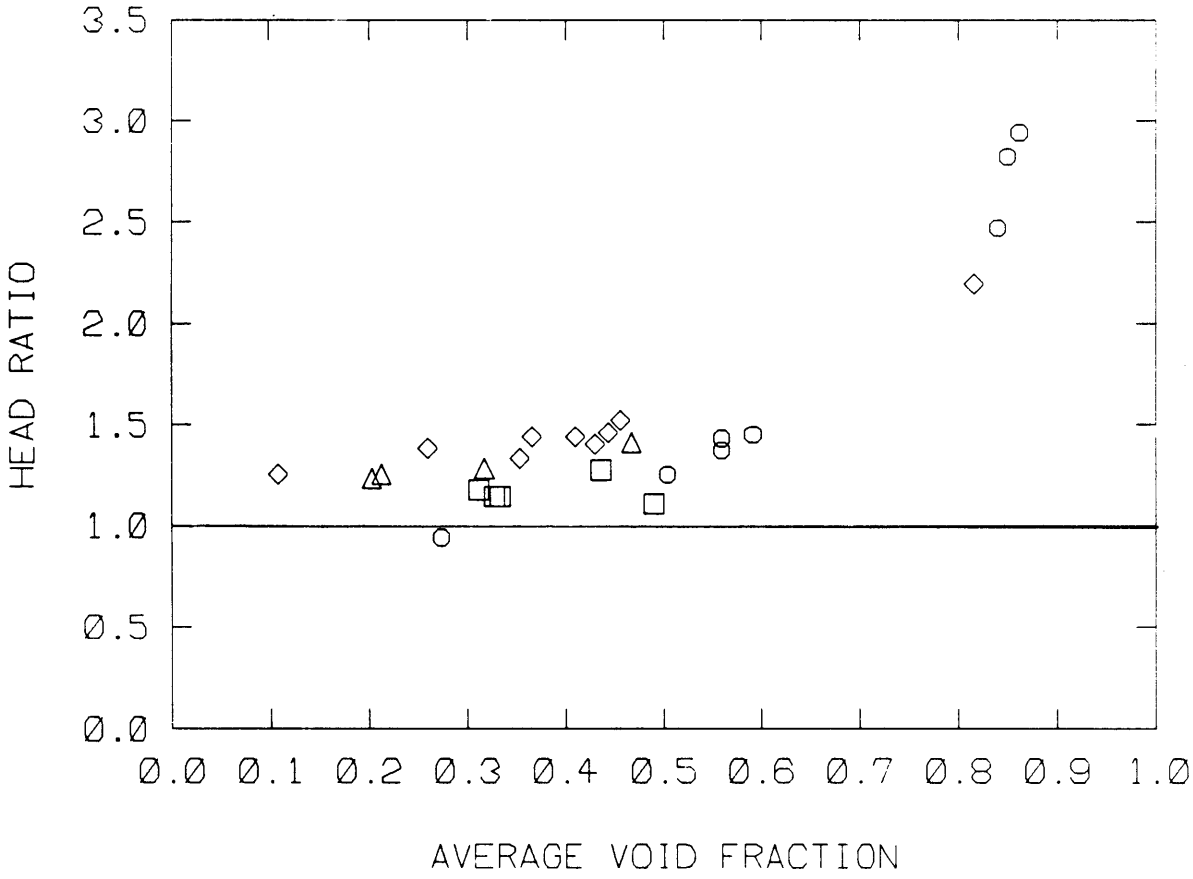

□ -0.67 < ϕ < -0.36
△ -0.24 < ϕ < -0.17
◇ -0.16 < ϕ < -0.08
○ -0.06 < ϕ < -0.01

820 < p < 1160 psi

FIGURE 3-14: HEAD RATIO ψ'_{tp}/ψ'_{sp} VS. AVERAGE VOID FRACTION $\alpha_{avg'}$ SECOND QUADRANT, CORRELATED BY FLOW COEFFICIENT ϕ

3.6. Third-Quadrant Results

The C-E steady-state, third-quadrant flow data appear in Appendix B, and the correlating parameters for two-phase performance appear in Appendix C . The least-squares polynomial fit used for single-phase performance was

$$\psi'_{sp} = 0.2760 - 3.412\phi + 28.30\phi^2 - 41.88\phi^3 + 97.45\phi^4$$

for the flow coefficient range

$$0.06 < \phi < 0.30$$

with a root-mean-square error in ψ'_{sp} of 0.0131 . The single-phase plot appears in Figure 3-15.

Theoretical performance was calculated using equation (2-14). A plot of the two-phase points and their relation to the theoretical and single-phase performance curves is given in Figure 3-16. Plots of head-loss ratio and head ratio against void fraction for the third quadrant are given in Figures 3-17 and 3-18, respectively.

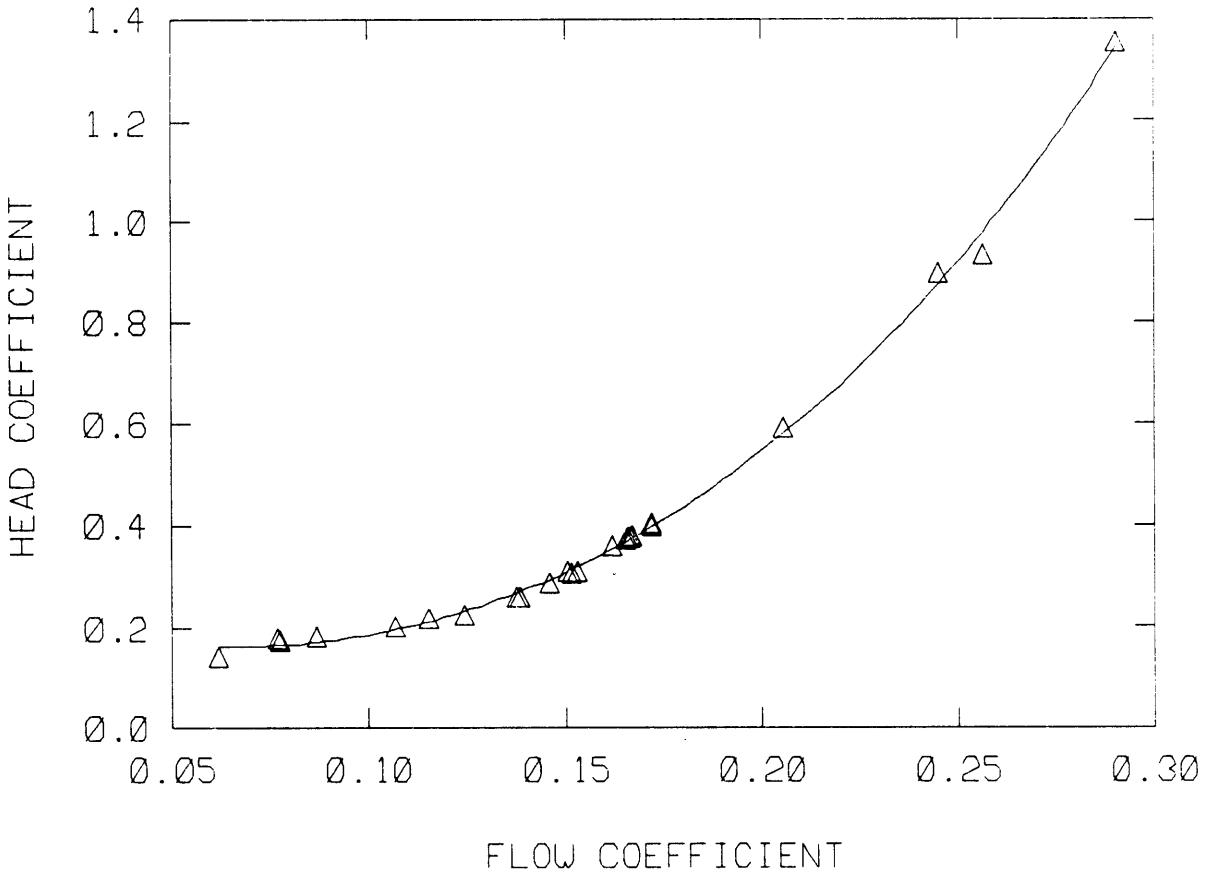

FIGURE 3-15: HEAD COEFFICIENT ψ' VS. FLOW COEFFICIENT ϕ, THIRD QUADRANT, SINGLE PHASE

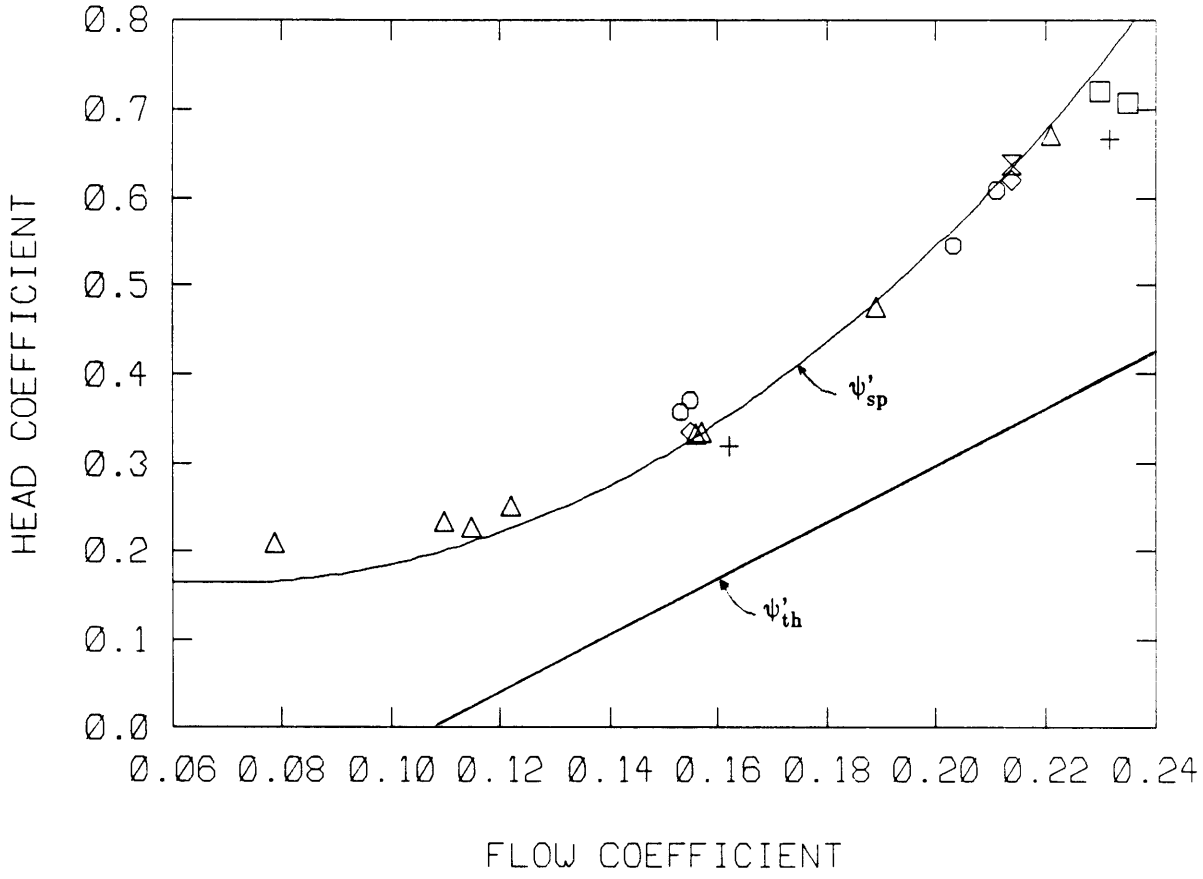

$\ast$ $0.0 < \alpha_{avg} < 0.1$
$+$ $0.1 < \alpha_{avg} < 0.2$
$\square$ $0.2 < \alpha_{avg} < 0.3$
$\triangle$ $0.3 < \alpha_{avg} < 0.5$
$\diamond$ $0.5 < \alpha_{avg} < 0.7$
$\circ$ $0.7 < \alpha_{avg} < 0.9$
$\boxtimes$ $0.9 < \alpha_{avg} < 1.0$

$520 < p < 1010$ psi

FIGURE 3-16: HEAD COEFFICIENT ψ' VS. FLOW COEFFICIENT ϕ, THIRD QUADRANT, TWO PHASE

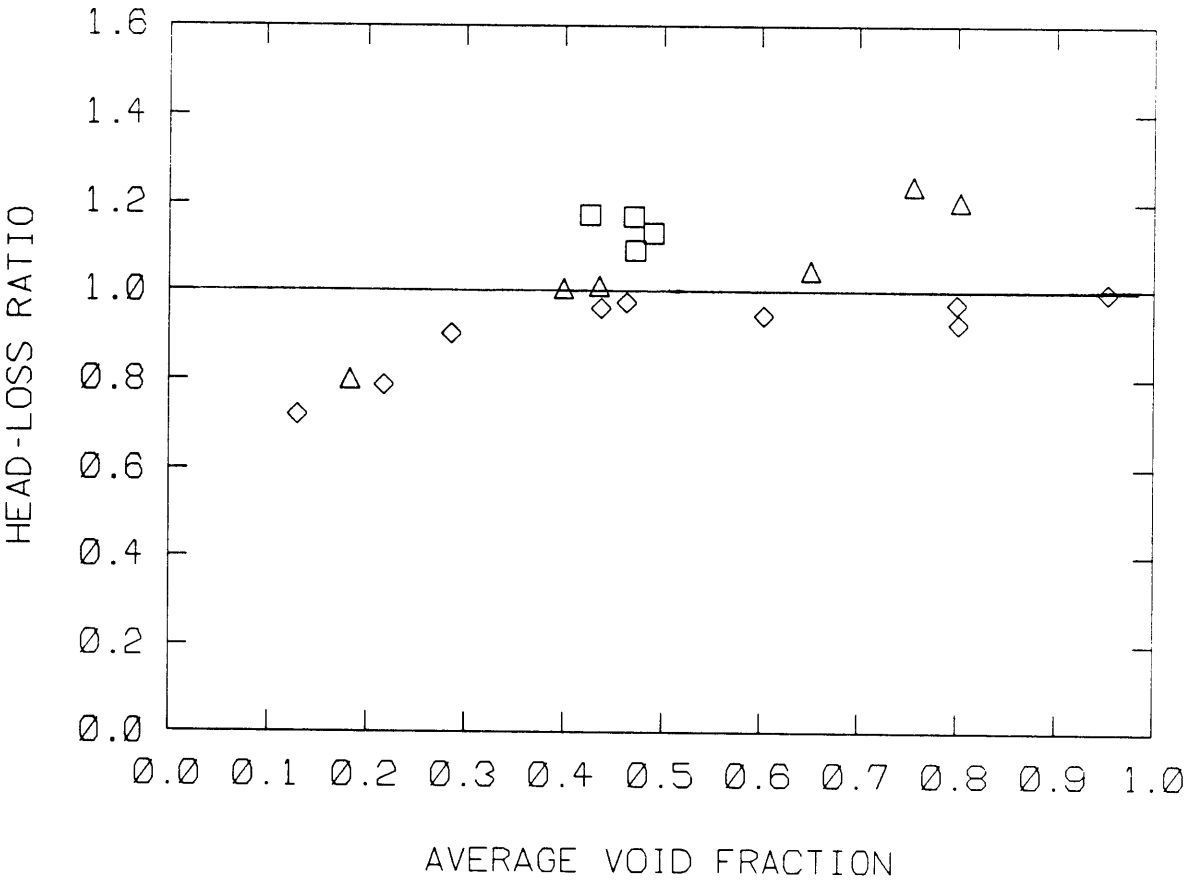

□ $0.08 < \phi < 0.12$
△ $0.15 < \phi < 0.16$
◇ $0.19 < \phi < 0.24$

$520 < p < 1010$ psi

FIGURE 3-17: HEAD-LOSS RATIO H^* VS. AVERAGE VOID FRACTION α_{avg}, THIRD QUADRANT, CORRELATED BY FLOW COEFFICIENT ϕ

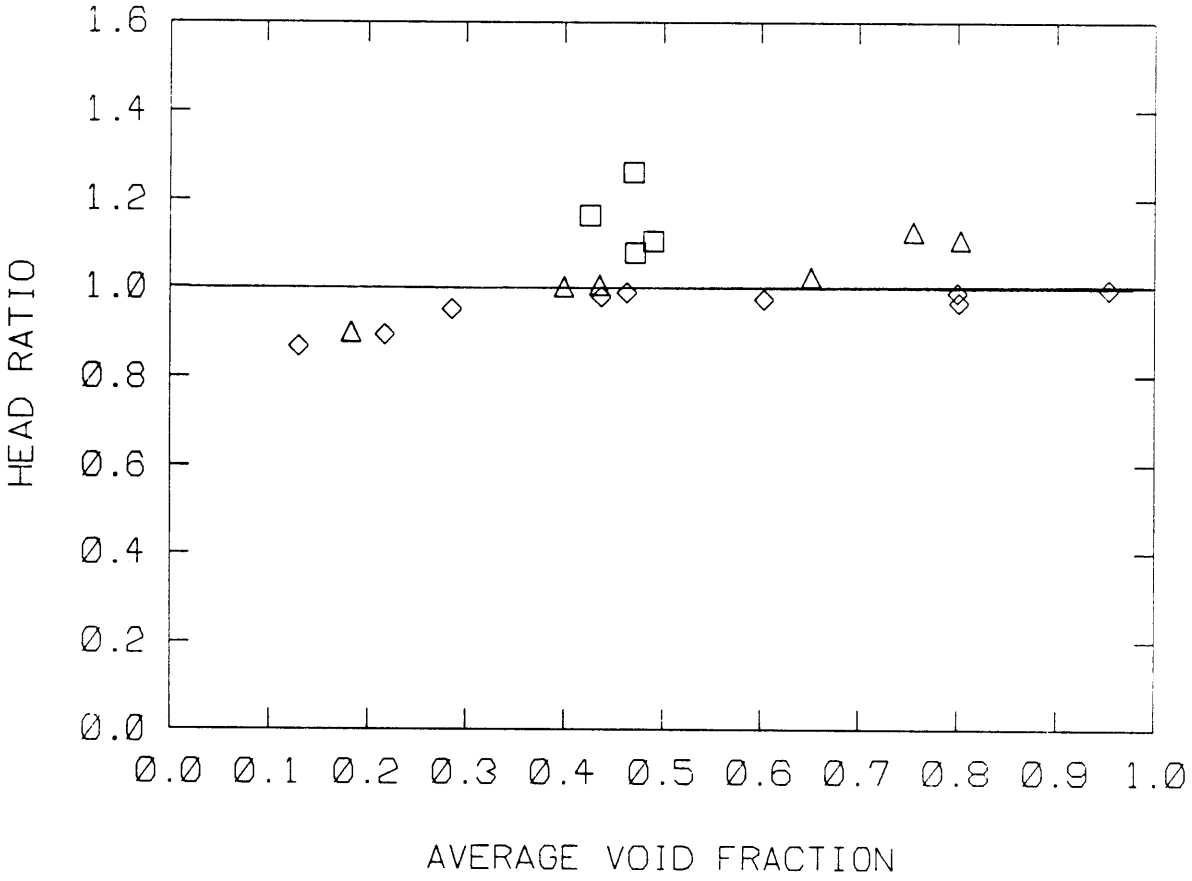

□ $0.08 < \phi < 0.12$
△ $0.15 < \phi < 0.16$
◇ $0.19 < \phi < 0.24$

$520 < p < 1010$ psi

FIGURE 3-18: HEAD RATIO ψ'_{tp}/ψ'_{sp} VS. AVERAGE VOID FRACTION $\alpha_{avg'}$ THIRD QUADRANT, CORRELATED BY FLOW COEFFICIENT ϕ

4. INTERPRETATION OF RESULTS

4.1. General Observations

The nature of the head-loss ratio is best illustrated by the two-phase plots of head coefficient against flow coefficient where the theoretical and single-phase performance curves have been included (Figures 3-4, 3-5, 3-13, and 3-16). The theoretical performance provides a geometrically-related reference from which to normalize the two-phase flow characteristics. The magnitude of the head-loss ratio is affected by the "distance" from the single-phase curve to the theoretical curve at a given flow coefficient as well as by the distance from the two-phase point. Since the difference between ψ'_{sp} and ψ'_{th} is greatest at higher flow-coefficient magnitudes (for all three quadrants), we can expect H^* to be closer to unity at high ϕ regardless of any material changes in the two-phase flow physics. Similarly, we can expect the head-loss ratio to be largest for two-phase points at flow coefficients where the theoretical and single-phase characteristics are close in value (at low and design-point flow coefficients). Therefore, although the two-phase physics at different flow regimes does affect the head-loss ratio magnitude, a significant effect is "artificially" created by the theoretical performance formulation (specifically, from the constant-slip-factor assumption).

The magnitude of the head ratio, ψ'_{tp}/ψ'_{sp} , for a given two-phase point is determined by the single-phase head-coefficient value in addition to the actual two-phase flow degradation. A problem in correlating by head ratio in the first quadrant is that the head ratio will become very large or negative at flow coefficients near where the head coefficient becomes zero. The head-loss ratio, however, avoids any problem in this region because of its definition and the fact that the theoretical line will never cross the single-phase curve.

In the second-quadrant results, the theoretical performance line intersected the single-phase performance curve (see Figure 3-13), causing large and negative head-loss ratios (Appendix C). Even if the theoretical line had only come close to the single-phase curve, the

head-loss-ratio correlation would have been adversely affected. Obviously, the theoretical relation used was not appropriate. The polynomial fit of the single-phase data was strongly quadratic, emphasizing that the second quadrant is almost entirely a dissipative region. In the formulation of the second-quadrant theoretical equation (2-13), the pump was treated as a performance machine; evidently, such a model does not adequately represent the true, dissipative second-quadrant performance. (Under the constant-inlet-flow-angle or straight-line assumption, though, the model was close to the actual characteristics). Two-phase correlation by the ratio of head losses is questionable in a quadrant where the performance is characterized only by losses.

The head-loss ratio correlated the first-quadrant two-phase data well. There was a significant amount of data with which meaningful curves were generated, although more data would be required to better complete the desired correlation ranges. The effects of system pressure and parameter variations from pump inlet to outlet for the first quadrant and the comparison of the results with other works are discussed in the next sections.

Insufficient two-phase data were available in the second and third quadrants to determine whether a correlation model, empirical or semi-empirical, is necessary at all. Indeed, the third-quadrant two-phase points all fell close to the single-phase performance curve, causing both the head-loss ratio and the head ratio to be near unity. This fact supports the accuracy of the measurement of two-phase density and the calculation of total head used in this analysis. Because of the uncertainty involved in the formulation of the theoretical performance, head ratio would be a better correlation parameter for the second and third quadrants.

The C-E data do exhibit a considerable amount of scatter. Often the reasons are because of the physical nature of two-phase flow: unsteady flow oscillations, non-uniform phase distributions, and irregular transitions of flow regime. Uncertainties in measurements by the instrumentation also amalgamated to diminish the accuracy of the reduced data. A

full investigation of the C-E data scatter, anomalies, and uncertainties was conducted by Kennedy, et al. [1980]. Dominant trends in head degradation related to void fraction, flow rate, and pressure were quite apparent despite data scatter. Subtle effects in two-phase pump performance (impeller speed and bubble-scale effects, for instance) would be difficult to discern from the C-E data.

4.2. Effect of System Pressure

The head-loss-ratio plot against void fraction for flows near the first-quadrant best-efficiency point ($\phi_{be} = 0.150$) correlated by system pressure, Figure 3-9, clearly illustrates the effect of the system pressure on two-phase pump performance. The two-phase head-degradation effects are enhanced at lower pressures because there is a greater difference between the respective liquid and vapor densities at lower saturation pressures. The density difference amplifies such two-phase mechanisms as fluid centrifugal forces and bubble drag forces. Contrarily, higher pressures suppress the head-degradation effects. Judging from Figure 3-9, head-loss-ratio magnitudes can be expected to decrease gradually for system pressures greater than 1250 psi (8600 kPa) and to increase in some way for pressures less than 450 psi (3100 kPa).

System pressure must be included as a parameter in any head-degradation correlation of steam/water two-phase flow. However, system pressure is probably not as important for the correlation of non-condensible gas/water flows (so long as cavitation is avoided). For such flows, the pressure does not affect the gas/liquid density ratio in the same manner as for steam/water flows. Also, without condensation of vapor, density and void fraction will not vary significantly through the pump. The effect of these variations on the C-E head-degradation correlations is discussed below.

4.3. Effect of Pump Inlet-to-Outlet Variations

The pressure variations in the two-phase flow traversing the pump cause constant adjustments of the thermodynamic equilibrium between the liquid water and steam. Two-phase density, volumetric flow rate, and void fraction vary from pump inlet to outlet. As explained in Chapter 3, the effects of density and flow rate variations were moderated by utilizing pump average values in the analysis. However, Figure 3-10 shows the result of correlating H^* to the upstream void fraction for first-quadrant flows near the best-efficiency point. By comparison with the plot against average void fraction, Figure 3-9, we observe that the shape of the head-loss-ratio curve differs most in the low void fraction region, $0.0 < \alpha < 0.3$. Vapor condensation accounts for the marked difference in this region. Void fractions of as much as 10% at pump inlet can completely vanish by pump outlet due to condensation prompted by large pressure changes (small head degradation). At higher void fractions, the pump head is so degraded that void fraction does not vary as much, and the correlation curve shapes are similar.

The difference between the correlations by upstream and average void fraction, at least at the flow-coefficient range shown, is significant enough that it should not be neglected when using the correlations for predictive purposes. When only upstream data are available, predictions could be made through utilizing some empirical correction of upstream void fraction and then entering the correlation curves plotted against average void fraction. Such an empirical correction, if workable, would eliminate the need for two sets of correlation curves.

4.4. Comparison with Other Works

The general shape of the head-loss-ratio curves for the first quadrant (Figures 3-6 through 3-10) agree well with curves generated by other MIT authors (Chan [1977], Manzano

[1980], Paik [1982], and Paran [1983]), and the physical reasons for the qualitative shape have been discussed elsewhere. However, the magnitudes of the head-loss ratios for similar flow-coefficient ranges do not agree well. Two reasons for these quantitative discrepancies are that different flow media were used (air/water (Manzano, Paran) or freon (Paik)) and that the overall pump efficiencies for each test system differed. Quantitative differences also exist for the head-ratio correlation. Because of these discrepancies, confidence in the application of the C-E data to pump systems that are not similar is diminished.

The magnitudes of H^* were greatest at the lowest flow coefficients and decreased with increasing flow coefficient up to and beyond the best-efficiency flow, ϕ_{be}. Manzano's results agreed with this trend, but some applications by Wilson, et al. [1979] showed that the largest head-loss ratios occurred near ϕ_{be}. Certainly the smallest single-phase losses occur at the design point, but apparently there can be significant increases in the two-phase losses at low flow coefficients. The trend of decreasing head degradation with increasing flow coefficient was also noted on a 1/20-scale model pump tested by Creare/EPRI. Here, Patel and Rundstadler [1978] observed the formation of larger voids within the pump during low-flow-coefficient operation. The existence and effect of these larger voids for a given pump most likely depends on its specific speed and geometric scale.

The effects of vapor-bubble scale relative to the pump geometric scale have been analyzed or noted by Rundstadler and Dolan [1978], Murakami and Minemura [1978], and Furuya [1984], among others. The extent of the dependence of the head degradation on scale needs to be determined in order for the C-E results to be considered valid for the full-scale reactor cooling system.

5. CONCLUSIONS AND RECOMMENDATIONS

5.1. Usefulness of C-E Data

As a data base for evaluating improved head-degradation models of two-phase pump flow, the C-E data contained too much scatter, uncertainty, and system dependence. Only rough trends can be observed and correlated; subtle effects that a new model might attempt to incorporate would be obfuscated. For the evaluation of the semi-empirical MIT model, the C-E data trends have provided added insight. The most positive aspect of the C-E test program is that the test system was a *scale model* of a currently-employed reactor coolant pump and tests were run near actual system conditions. Therefore, for LOCA predictive purposes, the C-E data yield the most justifiable correlations at present. Application to other pumps of *similar* size and specific speed should also be effective.

5.2. Applicability of MIT Model

This research has confirmed the head-loss-ratio method as an acceptable means of correlating pump head degradation in two-phase flow, subject to the recommendations listed below. There are, however, still too many factors which render the correlation pump-specific. These factors include pump efficiency, geometric scale, inlet-piping configuration, and pump specific speed (centrifugal, mixed-flow, etc.). The MIT semi-empirical model was developed as an attempt to understand and to distinguish some of the two-phase pump-flow phenomena, but there yet exists a preponderance of empiricism in its application.

5.3. Recommendations for Model Use

As a result of this application of the MIT semi-empirical model to the C-E data, the following recommendations for use of the model are made.

- Unless an analytical formulation of slip factor, μ, is developed which can confidently be applied to different pumps, a constant slip factor based on the design point, μ_{be}, should be utilized. Otherwise, the H^* correlation results become less reliable for predictive purposes.

- Head-loss ratio is an acceptable correlation method for the first quadrant, but its use in the second and third quadrants is disputable. For these latter quadrants, the primary difficulty is formulating an acceptable theoretical-head-coefficient relation. The purely empirical correlating factor ψ'_{tp}/ψ'_{sp} can be used with greater success in the second and third quadrants.

- System pressure must be included as a primary correlation parameter along with flow coefficient, at least for cases where the flow contains a condensible vapor.

- For the purpose of predicting two-phase pump performance involving a condensible vapor, a distinction should be made between upstream and average void fraction for best results.

APPENDIX A

C-E TEST PUMP DIMENSIONAL DATA

The following geometric parameters are required in the analytical model for correlation in the first, second, and third quadrants. Figure A-1 illustrates the notation.

Shroud radius at impeller inlet, r_{1s}

Hub radius at impeller exit, r_{1h}

Radii at impeller exit, r_{2o} and r_{2i}

Blade width at impeller exit, b_2

Blade thickness at impeller exit, t_2

Blade angle at impeller exit, β'_2

Radius at diffuser inlet, r_3

Blade width at diffuser inlet, b_3

Blade angle at diffuser inlet, α_3

Number of impeller blades, z

For the C-E test pump, we have the following corresponding dimensions.

$r_{1s} = 3.11$ in. (78.9 mm)

$r_{1h} = 1.42$ in. (36.1 mm)

$r_{2o} = 4.188$ in. (106.4 mm)

$r_{2i} = 3.688$ in. (93.7 mm)

$b_2 = 2.12$ in. (53.8 mm)

$t_2 = 0.200$ in. (5.1 mm)

$\beta'_2 = 31°$ [$\beta'_{2o} = 30°$, $\beta'_{2i} = 32°$]

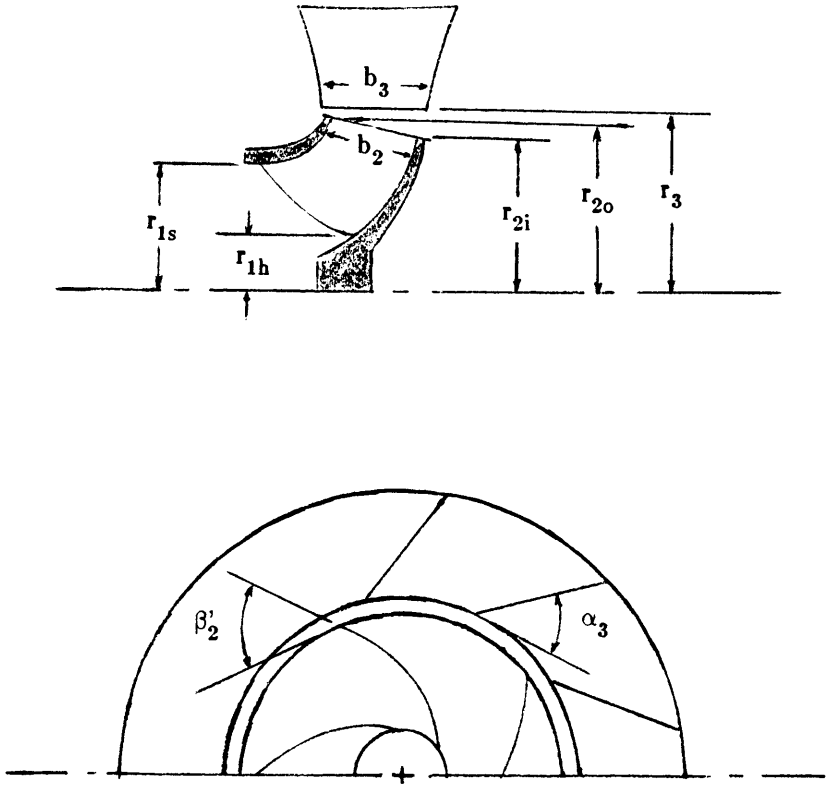

FIGURE A-1: NOTATION OF PUMP DIMENSIONS AND ANGLES

$r_3 = 4.36$ in. (110.8 mm)

$b_3 = 2.65$ in. (67.3 mm)

$\alpha_3 = 51°$

$z = 5$

The dimensions at the impeller exit (station 2) differ somewhat from those values originally reported in the MIT/EPRI report (Wilson, et al. [1979]). These corrected dimensions come as the result of a "hands-on" inspection of the actual C-E test pump impeller, courtesy of Combustion Engineering. The most notable emendation is of the blade angle at the impeller exit which had been reported as 23°.

The geometry of the 1/20-scale pump used in the Creare/EPRI test program (Rundstadler, et al. [1977]) was based on inspections and rubber molds of the C-E test pump. The Creare pump dimensions (obtained from an inspection report and blade drawing courtesy of Creare) compared well with the dimensions given above, except for the exit blade angle. Apparently, the 1/20-scale-pump impeller-exit blade angle varied from $\beta'_{2o}=20°$ to $\beta'_{2i}\approx 37°$. Although the average value of this angle is close to the C-E pump average value, the variation from outer- to inner-shroud is considerably different.

Two derived dimensions used in the analysis are the mean effective radius at impeller exit,

$$r_{2,m} = \sqrt{(r_{2o}^2 + r_{2i}^2)/2} = 3.946 \text{ in.} \quad (100.2 \text{ mm})$$

and the net flow area at impeller exit (excluding the 7.8% blade blockage),

$$A_2 = (2\pi r_{2,avg} - \frac{z t_2}{\sin \beta'_2}) b_2 = 48.34 \text{ in.}^2 \quad (31190 \text{ mm}^2)$$

The cold-water rated (best-efficiency) conditions of the C-E test pump are as follows.

$Q_{rated} = 3500$ gpm (0.221 m^3/s)

$H_{rated} = 252$ ft (76.8 m)

$N_{rated} = 4500$ rpm

$N_s = 4200$

[ρ=62.3 lbm/ft^3 (998 kg/m^3)]

These rated values can be expressed in terms of head and flow coefficients for the purpose of relating the pump performance curves to the best-efficiency point (eg., producing homologous ratios).

$\phi_{rated} = 0.150$

$\psi'_{rated} = 0.338$

APPENDIX B

C-E STEADY-STATE FLOW DATA

Data for each test point were obtained from the C-E steady-state one-page printouts (Kennedy, et al. [1980]). Every available two-phase test point is included here that was part of the C-E steady-state test matrix, except for those points taken during low-pressure (less than 200 psi (1400 kPa)) or locked-impeller (zero speed) conditions. Low-pressure points invloved undesirably low two-phase densities which made calculations of H_o inaccurate for the given precision of the C-E data, and the flow coefficient is undefined for zero-speed conditions.

Each test point is labeled using the C-E-assigned number. Volumetric flow rate (Q), void fraction (α), fluid density (ρ), and system pressure (p) are arithmetic averages of the upstream and downstream measurements. The pump static-pressure rise (Δp) was taken from suction flange to discharge flange. The total head (H_o) was calculated using equation (2-6). The upstream and downstream fluid velocities were included in this calculation but are not shown here, and the suction-to-discharge elevation change was + 1.0 ft (+ 0.3 m). The flow quality (x) was based on upstream measurements just before the mixing of the individual liquid and vapor flows. The data are arranged by increasing or decreasing flow coefficient, depending on the quadrant.

B.1. First-Quadrant, Single-Phase Data

Only those single-phase data sufficient for developing the single-phase performance curve are included here; more first-quadrant, single-phase data were available.

TEST #	Q gpm	α_{avg}	N rpm	ρ lbm/ft^3	Δp psi	H_o ft	x_{ups}	p psi	ϕ	ψ'
336	40	0.000	5809	46.72	193.12	596.3	0.000	1308	0.0013	0.4794
326	149	0.000	4491	60.67	150.77	358.8	0.000	270	0.0064	0.4827
365	152	0.000	2240	61.60	29.31	69.5	0.000	25	0.0130	0.3759
637	340	0.000	4479	61.53	149.87	351.8	0.000	103	0.0146	0.4758
636	181	0.000	2237	61.57	36.69	86.8	0.000	44	0.0156	0.4707
717	337	0.000	3869	46.41	83.71	260.7	0.000	1058	0.0168	0.4725
638	803	0.000	4472	61.48	143.35	336.7	0.000	93	0.0346	0.4569
325	1070	0.000	4492	60.62	142.68	339.8	0.000	242	0.0459	0.4570
256	1502	0.000	4456	60.93	129.44	306.9	0.000	167	0.0650	0.4193
209	1542	0.000	4497	47.18	101.33	310.2	0.000	1070	0.0661	0.4161
214	1638	0.000	4501	47.23	99.51	304.2	0.000	1059	0.0702	0.4075
780	1015	0.000	2548	48.53	32.50	97.4	0.000	882	0.0768	0.4070
649	977	0.000	2252	49.17	25.10	74.5	0.000	877	0.0836	0.3984
648	1006	0.000	2263	49.11	25.06	74.4	0.000	876	0.0857	0.3942
668	999	0.000	2240	48.58	24.23	72.8	0.000	879	0.0860	0.3934
625	1002	0.000	2243	48.76	24.39	72.9	0.000	883	0.0861	0.3933
580	1008	0.000	2244	49.46	24.82	73.2	0.000	879	0.0866	0.3943
695	1017	0.000	2242	48.54	24.26	72.9	0.000	879	0.0874	0.3937
366	1040	0.000	2239	61.50	31.00	73.6	0.000	46	0.0895	0.3982
578	1094	0.000	2250	49.36	24.62	72.7	0.000	880	0.0937	0.3898
324	2184	0.000	4485	60.66	122.77	292.3	0.000	228	0.0939	0.3942
676	2342	0.000	4582	46.31	63.58	198.8	0.000	989	0.0985	0.2570
846	2432	0.000	4510	46.25	66.23	207.3	0.000	998	0.1039	0.2765
701	2510	0.000	4483	46.21	68.75	215.4	0.000	1015	0.1079	0.2908
255	2770	0.000	4450	61.07	114.77	271.6	0.000	112	0.1200	0.3721
210	2897	0.000	4488	46.91	90.56	278.8	0.000	1038	0.1244	0.3756
323	2973	0.000	4476	60.72	115.94	275.7	0.000	203	0.1280	0.3734
211	3473	0.000	4486	46.71	77.47	239.7	0.000	1032	0.1492	0.3231
845	3524	0.000	4491	45.96	76.69	241.1	0.000	1090	0.1513	0.3244
777	2217	0.000	2545	48.08	21.87	66.4	0.000	955	0.1679	0.2781
212	3984	0.000	4490	46.92	64.83	199.6	0.000	1044	0.1710	0.2686
579	1999	0.000	2243	48.85	16.60	49.8	0.000	875	0.1718	0.2685
650	2015	0.000	2253	48.38	16.42	49.8	0.000	870	0.1724	0.2660
624	2014	0.000	2241	48.41	16.05	48.5	0.000	882	0.1732	0.2622
696	2018	0.000	2242	48.19	16.02	48.8	0.000	863	0.1735	0.2634
669	2021	0.000	2240	48.17	15.88	48.4	0.000	867	0.1739	0.2616
321	4080	0.000	4482	60.92	79.96	189.7	0.000	150	0.1755	0.2562
671	2049	0.000	2241	48.03	15.63	47.8	0.000	862	0.1763	0.2580

TEST #	Q gpm	α_{avg}	N rpm	ρ lbm/ft^3	Δp psi	H_o ft	x_{ups}	p psi	ϕ	ψ'
367	2054	0.000	2239	61.39	19.78	47.3	0.000	80	0.1768	0.2561
335	4995	0.000	5367	44.78	72.42	233.6	0.000	1229	0.1794	0.2201
322	4327	0.000	4488	60.84	56.22	133.8	0.000	123	0.1859	0.1802
343	4631	0.000	4499	44.88	40.64	131.1	0.000	1205	0.1984	0.1758
778	2624	0.000	2546	48.01	15.88	48.5	0.000	939	0.1986	0.2030
213	4729	0.000	4502	46.69	43.08	133.5	0.000	1029	0.2025	0.1788
581	2662	0.000	2244	48.65	6.94	21.3	0.000	864	0.2286	0.1150
627	2683	0.000	2245	45.91	5.64	18.4	0.000	1138	0.2303	0.0990
623	2689	0.000	2244	48.22	5.88	18.3	0.000	868	0.2310	0.0987
697	2710	0.000	2242	47.97	5.68	18.0	0.000	868	0.2330	0.0972
672	2728	0.000	2248	47.91	5.31	16.9	0.000	849	0.2339	0.0906
257	3192	0.000	2604	61.17	5.75	14.4	0.000	108	0.2363	0.0578
670	2758	0.000	2242	47.99	4.67	14.9	0.000	850	0.2371	0.0807
368	3001	0.000	2245	61.20	-1.45	-2.6	0.000	104	0.2576	-0.0137
779	3441	0.000	2553	47.91	-0.14	0.5	0.000	904	0.2598	0.0022
698	3031	0.000	2246	47.89	-0.97	-1.9	0.000	856	0.2601	-0.0104
674	3107	0.000	2255	48.45	-2.30	-6.0	0.000	845	0.2656	-0.0319
584	3114	0.000	2237	57.30	-3.42	-7.8	0.000	176	0.2683	-0.0421
618	3195	0.000	2236	52.72	-6.87	-18.0	0.000	400	0.2754	-0.0976
583	3248	0.000	2240	52.70	-6.44	-16.8	0.000	420	0.2795	-0.0908
619	3246	0.000	2237	52.73	-8.16	-21.5	0.000	397	0.2797	-0.1165
585	3289	0.000	2255	57.30	-9.61	-23.3	0.000	166	0.2811	-0.1245
587	3312	0.000	2265	60.63	-36.56	-86.0	0.000	63	0.2819	-0.4548
582	3349	0.000	2254	47.58	-6.61	-19.3	0.000	954	0.2864	-0.1033
617	3373	0.000	2240	57.30	-25.38	-62.9	0.000	125	0.2902	-0.3404
311	3381	0.000	2243	45.35	-8.47	-26.1	0.000	1202	0.2905	-0.1407
616	3390	0.000	2244	60.90	-39.98	-93.7	0.000	66	0.2912	-0.5048
699	3411	0.000	2254	48.26	-9.31	-26.9	0.000	862	0.2917	-0.1437
673	3424	0.000	2259	48.31	-10.85	-31.5	0.000	834	0.2922	-0.1675
586	3447	0.000	2253	57.30	-18.99	-46.9	0.000	155	0.2949	-0.2505
844	3453	0.000	2251	48.36	-10.63	-30.8	0.000	844	0.2957	-0.1651
588	3460	0.000	2251	60.64	-46.21	-108.9	0.000	70	0.2963	-0.5832
369	3490	0.000	2266	61.06	-43.58	-101.8	0.000	69	0.2968	-0.5382
675	3497	0.000	2255	45.96	-13.22	-40.6	0.000	1096	0.2989	-0.2166
700	3502	0.000	2251	45.98	-11.82	-36.2	0.000	1123	0.2999	-0.1939
843	3536	0.000	2244	48.11	-13.36	-38.9	0.000	859	0.3038	-0.2096
260	3238	0.000	2009	60.88	-28.66	-66.9	0.000	90	0.3106	-0.4494
342	3707	0.000	2264	45.06	-18.80	-59.3	0.000	1200	0.3156	-0.3142
689	2769	0.000	1619	52.70	-15.73	-41.7	0.000	360	0.3296	-0.4316
842	3517	0.000	2040	48.20	-20.09	-58.9	0.000	850	0.3323	-0.3843
798	3393	0.000	1967	48.22	-18.39	-54.0	0.000	859	0.3325	-0.3786
258	3214	0.000	1842	61.01	-28.63	-66.6	0.000	88	0.3363	-0.5327
841	3063	0.000	1751	48.28	-15.34	-44.7	0.000	863	0.3372	-0.3957
310	3958	0.000	2251	45.33	-28.63	-90.1	0.000	1179	0.3389	-0.4826
799	3079	0.000	1745	48.14	-15.57	-45.6	0.000	858	0.3401	-0.4064

TEST #	Q gpm	α_{avg}	N rpm	ρ lbm/ft^3	Δp psi	H_o ft	x_{ups}	p psi	ϕ	ψ'
840	2755	0.000	1556	47.91	-13.21	-38.6	0.000	852	0.3413	-0.4326
797	2731	0.000	1542	47.89	-12.61	-37.0	0.000	861	0.3414	-0.4217
259	3215	0.000	1809	60.96	-28.61	-66.6	0.000	87	0.3426	-0.5524
796	2053	0.000	1119	47.82	-7.63	-22.0	0.000	865	0.3537	-0.4768
839	1936	0.000	1047	48.13	-7.22	-20.6	0.000	859	0.3564	-0.5089
643	1540	0.000	798	49.56	-8.72	-24.3	0.000	716	0.3720	-1.0373
688	798	0.000	400	56.93	-2.09	-4.2	0.000	144	0.3846	-0.7199
830	902	0.000	443	57.18	-2.46	-5.2	0.000	160	0.3923	-0.7232
838	1011	0.000	472	48.50	-2.98	-7.8	0.000	869	0.4127	-0.9526
795	1035	0.000	483	47.92	-2.96	-7.9	0.000	870	0.4129	-0.9205
661	563	0.000	255	57.17	-1.46	-2.7	0.000	99	0.4252	-1.1198
663	749	0.000	336	52.84	-2.03	-4.6	0.000	385	0.4294	-1.0980
639	608	0.000	270	57.30	-1.84	-3.6	0.000	166	0.4341	-1.3470
358	3201	1.000	4492	2.25	3.82	241.1	1.000	1001	0.1373	0.3241
268	3421	1.000	4494	1.04	1.27	173.0	1.000	479	0.1467	0.2325
309	4929	1.000	4492	2.23	1.68	107.1	1.000	993	0.2115	0.1440
302	2633	1.000	2266	2.74	0.23	10.8	1.000	1189	0.2239	0.0571
300	3081	1.000	2266	2.23	-0.16	-11.1	1.000	993	0.2621	-0.0585
357	3240	1.000	2249	2.25	-0.56	-38.5	1.000	998	0.2777	-0.2068
267	3398	1.000	2248	1.04	-0.71	-102.0	1.000	479	0.2914	-0.5478
301	3432	1.000	2267	2.24	-0.62	-39.9	1.000	995	0.2918	-0.2107
916	3582	1.000	2245	1.85	-0.54	-42.8	1.000	843	0.3075	-0.2303
315	7608	1.000	4522	0.98	-1.95	-286.3	1.000	447	0.3243	-0.3799
318	8059	1.000	4489	0.94	-3.10	-485.6	1.000	437	0.3461	-0.6539
319	8798	1.000	4490	0.96	-4.49	-683.9	1.000	446	0.3777	-0.9204
308	5010	1.000	2267	2.24	-3.91	-251.2	1.000	996	0.4260	-1.3262
822	5288	1.000	2249	0.64	-1.20	-278.6	1.000	301	0.4532	-1.4947
316	7735	1.000	2245	0.94	-7.07	-1086.6	1.000	438	0.6641	-5.8498
320	8262	1.000	2235	0.98	-8.59	-1274.1	1.000	454	0.7125	-6.9210

B.2. First-Quadrant, Two-Phase Data

TEST #	Q gpm	α_{avg}	N rpm	ρ lbm/ft^3	Δp psi	H_o ft	x_{ups}	p psi	ϕ	ψ'
289	160	0.283	4484	34.18	82.63	349.0	0.052	1018	0.0069	0.4710
287	146	0.211	2247	37.73	22.93	88.5	0.041	1013	0.0125	0.4754
1420	180	0.533	2240	22.89	5.10	33.1	0.048	989	0.0154	0.1792
920	368	0.844	4494	8.99	9.84	158.8	0.148	850	0.0158	0.2134
921	419	0.528	4479	23.05	29.17	183.4	0.052	1016	0.0180	0.2481
1417	228	0.589	2238	20.43	5.90	42.7	0.066	987	0.0196	0.2312
276	1316	0.821	6732	10.04	18.86	271.8	0.154	869	0.0377	0.1627
922	937	0.431	4482	27.27	36.53	193.9	0.040	1023	0.0403	0.2619
277	1549	0.855	6728	8.51	17.83	303.0	0.187	856	0.0444	0.1816
286	1259	0.362	4962	30.23	55.73	265.4	0.024	1029	0.0489	0.2925
285	1178	0.342	4530	31.11	52.93	245.2	0.022	1032	0.0501	0.3242
275	1261	0.820	4496	10.13	7.70	110.8	0.150	846	0.0541	0.1487
229	1378	0.464	4467	25.82	32.44	181.2	0.041	1004	0.0595	0.2464
362	1221	0.417	3749	27.87	21.22	110.9	0.046	1019	0.0628	0.2141
284	1206	0.340	3145	31.31	18.42	85.2	0.029	1007	0.0739	0.2337
271	3359	0.785	8589	11.71	38.48	470.3	0.130	869	0.0754	0.1730
228	1340	0.463	3149	25.93	11.96	66.8	0.045	1001	0.0820	0.1829
217	2095	0.343	4588	31.53	34.66	157.1	0.035	920	0.0880	0.2026
888	2084	0.177	4458	38.42	65.28	242.2	0.018	1021	0.0901	0.3307
281	2646	0.468	5575	25.66	43.91	243.9	0.041	1004	0.0915	0.2130
363	1222	0.417	2474	27.93	11.36	60.1	0.049	1008	0.0952	0.2663
226	2732	0.458	5495	26.16	44.13	241.1	0.035	1001	0.0958	0.2167
237	2252	0.503	4506	24.16	26.55	158.2	0.054	1000	0.0963	0.2115
270	3397	0.794	6778	11.26	19.50	248.6	0.136	856	0.0966	0.1468
239	2436	0.459	4493	26.10	27.65	152.3	0.045	996	0.1045	0.2047
339	2465	0.418	4533	27.89	31.09	160.6	0.038	1002	0.1048	0.2121
225	2474	0.416	4441	27.96	32.52	167.2	0.030	1010	0.1074	0.2300
334	4159	0.347	7328	30.84	106.09	477.2	0.024	1036	0.1094	0.2411
283	1284	0.445	2247	26.71	5.11	28.3	0.044	998	0.1102	0.1520
273	1304	0.821	2248	10.03	1.10	17.3	0.151	846	0.1118	0.0928
242	2614	0.411	4457	28.23	30.09	152.8	0.038	1000	0.1131	0.2087
571	3713	0.143	5854	39.07	100.86	360.0	0.001	1158	0.1223	0.2850
359	4271	0.358	6670	30.41	79.22	362.3	0.034	1029	0.1234	0.2210
338	3559	0.417	5484	27.90	48.19	246.0	0.038	1012	0.1251	0.2219
361	3362	0.379	5168	29.53	45.07	216.8	0.045	1023	0.1254	0.2203
719	1679	0.187	2578	38.29	9.27	35.6	0.029	968	0.1255	0.1452
720	1708	0.165	2573	39.29	10.89	40.5	0.027	969	0.1280	0.1661
279	3152	0.157	4682	39.25	62.46	222.6	0.030	1020	0.1298	0.2755
235	3120	0.450	4493	26.45	22.52	122.3	0.044	1007	0.1338	0.1644
243	3162	0.343	4496	31.22	31.16	141.8	0.030	996	0.1356	0.1903
988	3178	0.617	4500	20.09	6.16	45.8	0.036	487	0.1361	0.0614

TEST #	Q gpm	α_{avg}	N rpm	ρ lbm/ft^3	Δp psi	H_o ft	x_{ups}	p psi	ϕ	ψ'
223	3188	0.069	4471	43.26	72.03	234.1	0.017	1028	0.1375	0.3178
881	3232	0.144	4516	43.65	30.14	92.2	0.016	472	0.1379	0.1226
572	3226	0.021	4492	44.56	81.87	263.3	0.012	1157	0.1384	0.3541
264	3244	0.785	4501	11.74	2.92	36.0	0.084	481	0.1389	0.0482
967	3241	0.342	4494	33.75	18.01	73.6	0.016	487	0.1390	0.0989
959	817	0.462	1127	25.95	0.56	4.4	0.045	1004	0.1397	0.0935
1122	3253	0.991	4486	1.49	1.78	173.7	0.731	482	0.1398	0.2342
377	3254	0.051	4486	42.58	72.71	241.9	0.003	1222	0.1398	0.3261
234	3321	0.406	4487	28.39	26.27	132.5	0.038	1010	0.1427	0.1786
278	3328	0.182	4464	38.25	46.96	171.6	0.028	1007	0.1437	0.2336
269	3370	0.795	4480	11.23	5.13	66.8	0.136	851	0.1450	0.0903
1115	3395	0.126	4509	40.94	54.22	184.7	0.005	955	0.1451	0.2465
990	3376	0.132	4473	44.28	28.27	85.1	0.009	484	0.1455	0.1154
1116	3406	0.126	4504	40.98	56.49	192.4	0.005	970	0.1458	0.2573
354	3398	0.951	4491	4.40	4.80	159.8	0.469	1001	0.1458	0.2149
355	3406	0.913	4492	6.11	5.37	129.2	0.327	1002	0.1461	0.1738
1114	3447	0.146	4532	40.05	50.54	175.9	0.008	975	0.1466	0.2323
991	3399	0.144	4468	43.67	26.80	81.5	0.010	486	0.1466	0.1107
721	1961	0.288	2572	33.80	10.75	46.3	0.036	972	0.1469	0.1899
381	3442	0.245	4503	34.42	50.45	208.2	0.017	1210	0.1473	0.2786
346	3445	0.641	4496	18.09	10.90	89.3	0.084	1004	0.1477	0.1199
216	3462	0.183	4515	38.12	42.06	154.7	0.018	1019	0.1478	0.2059
992	3440	0.157	4484	43.01	24.86	76.7	0.011	486	0.1479	0.1035
347	3463	0.807	4507	10.76	6.63	91.4	0.174	1013	0.1481	0.1221
1113	3490	0.169	4536	39.19	45.40	161.4	0.009	951	0.1483	0.2129
911	3457	0.643	4490	18.17	7.90	64.1	0.074	852	0.1484	0.0863
387	3476	0.801	4495	10.98	5.76	78.7	0.169	843	0.1491	0.1056
215	3490	0.056	4500	43.79	68.03	218.3	0.004	1024	0.1495	0.2925
233	3501	0.376	4511	29.71	26.60	128.0	0.034	1010	0.1496	0.1707
333	6015	0.402	7744	28.56	67.94	328.0	0.040	1013	0.1497	0.1484
989	3521	0.656	4500	18.21	5.03	42.2	0.042	477	0.1508	0.0566
350	3502	0.123	4475	40.82	60.41	207.5	0.004	1020	0.1508	0.2812
313	3525	0.421	4486	27.79	21.17	110.5	0.037	994	0.1515	0.1490
379	3544	0.157	4483	38.05	52.79	195.8	0.010	1225	0.1524	0.2644
994	3584	0.904	4502	5.81	2.30	59.8	0.164	480	0.1534	0.0800
918	3577	0.953	4492	4.01	3.90	142.3	0.436	846	0.1535	0.1914
232	3599	0.296	4492	33.24	32.07	136.6	0.021	1004	0.1544	0.1837
1112	3651	0.240	4533	35.98	35.85	140.4	0.016	961	0.1552	0.1854
995	3631	0.951	4505	3.50	2.28	96.9	0.279	479	0.1554	0.1295
961	3629	0.420	4491	27.40	24.30	128.0	0.043	1113	0.1558	0.1722
344	3708	0.452	4503	26.41	16.02	89.0	0.040	999	0.1587	0.1191
993	3732	0.822	4506	9.91	2.31	36.7	0.089	474	0.1597	0.0491
332	5654	0.417	6728	27.92	45.97	233.1	0.044	1003	0.1620	0.1397
224	3950	0.364	4492	30.32	25.25	120.1	0.028	996	0.1695	0.1615
960	3995	0.498	4497	23.92	15.96	97.2	0.059	1178	0.1712	0.1305

TEST #	Q gpm	α_{avg}	N rpm	ρ lbm/ft^3	Δp psi	H_o ft	x_{ups}	p psi	ϕ	ψ'
987	4006	0.693	4502	16.34	3.12	30.6	0.049	479	0.1715	0.0410
238	2108	0.506	2247	24.05	1.78	12.2	0.057	995	0.1808	0.0656
919	3621	0.805	3811	10.78	2.75	39.1	0.141	846	0.1832	0.0731
903	3722	0.245	3754	35.55	16.82	68.5	0.021	1000	0.1911	0.1319
240	2240	0.452	2239	26.42	1.52	10.0	0.048	987	0.1929	0.0540
742	3934	0.503	3888	24.53	6.12	36.6	0.056	866	0.1950	0.0657
360	4657	0.426	4497	27.57	10.80	61.7	0.041	989	0.1996	0.0828
569	3274	0.056	3152	42.35	21.02	72.7	0.005	1217	0.2002	0.1985
740	3616	0.450	3443	26.83	5.71	31.6	0.051	902	0.2024	0.0723
739	2431	0.398	2249	29.04	1.63	9.2	0.050	937	0.2084	0.0496
241	2426	0.420	2241	27.85	1.22	8.2	0.043	992	0.2086	0.0443
738	2454	0.343	2244	31.53	2.79	13.8	0.043	934	0.2108	0.0744
958	3489	0.799	3167	11.14	1.06	16.1	0.164	996	0.2124	0.0437
726	2525	0.365	2262	30.50	1.25	7.1	0.041	947	0.2152	0.0376
280	2532	0.433	2266	27.26	0.36	3.3	0.042	994	0.2154	0.0172
292	2561	0.438	2248	27.04	1.65	11.2	0.043	993	0.2196	0.0603
331	5119	0.424	4482	27.67	1.01	16.5	0.048	980	0.2201	0.0223
274	1283	0.820	1122	10.12	-0.57	-6.7	0.153	849	0.2203	-0.1452
330	5163	0.432	4492	27.41	0.03	11.8	0.048	956	0.2215	0.0159
901	3653	0.245	3157	35.59	4.87	22.7	0.023	990	0.2230	0.0617
902	3717	0.374	3165	29.90	1.67	11.6	0.035	988	0.2264	0.0315
904	3732	0.674	3168	16.63	0.06	3.3	0.095	1002	0.2271	0.0090
1416	3970	0.250	3354	35.60	3.24	18.3	0.025	955	0.2281	0.0442
1415	3984	0.284	3357	34.09	1.61	12.0	0.027	949	0.2287	0.0289
900	3787	0.184	3159	38.28	3.55	16.7	0.019	995	0.2311	0.0455
314	5446	0.455	4495	26.30	-5.74	-17.0	0.051	986	0.2335	-0.0229
265	2762	0.876	2245	7.25	-1.32	-25.3	0.162	522	0.2372	-0.1360
737	2793	0.420	2252	28.05	-0.84	-2.8	0.053	938	0.2390	-0.0150
384	2782	0.725	2236	14.43	-0.72	-4.5	0.122	850	0.2398	-0.0243
773	3451	0.276	2554	34.46	-4.62	-16.7	0.030	947	0.2605	-0.0694
263	3137	0.772	2249	12.40	-3.56	-39.6	0.081	481	0.2689	-0.2123
1123	3137	0.990	2242	1.57	-0.14	-10.1	0.706	482	0.2697	-0.0547
297	3188	0.198	2256	38.62	-13.45	-44.1	0.021	826	0.2724	-0.2350
266	3234	0.940	2248	4.04	-1.76	-65.9	0.285	482	0.2773	-0.3539
570	4686	0.120	3158	39.70	-15.96	-45.5	0.018	1205	0.2860	-0.1239
1394	5470	0.482	3675	25.30	-28.13	-137.1	0.053	936	0.2869	-0.2755
1395	5361	0.468	3562	25.96	-28.04	-132.2	0.051	917	0.2901	-0.2828
353	3380	0.951	2246	4.43	-1.63	-50.0	0.467	1001	0.2901	-0.2689
230	3415	0.449	2243	26.62	-13.97	-70.9	0.045	978	0.2935	-0.3825
356	3451	0.911	2249	6.16	-2.49	-55.2	0.324	997	0.2958	-0.2962
386	3454	0.800	2247	11.03	-3.25	-38.8	0.169	843	0.2963	-0.2086
1396	5329	0.466	3428	26.06	-31.02	-147.6	0.051	916	0.2996	-0.3407
221	3527	0.179	2253	38.50	-28.63	-103.9	0.023	991	0.3017	-0.5556
383	3504	0.794	2239	11.42	-4.91	-58.5	0.207	1195	0.3017	-0.3167

TEST #	Q gpm	α_{avg}	N rpm	ρ lbm/ft^3	Δp psi	H_o ft	x_{ups}	p psi	ϕ	ψ'
1414	4636	0.690	2957	16.11	-13.03	-107.1	0.086	767	0.3022	-0.3322
912	3522	0.669	2243	17.01	-6.76	-53.6	0.078	835	0.3027	-0.2888
345	3536	0.664	2246	17.07	-8.00	-64.0	0.091	999	0.3035	-0.3444
348	3568	0.807	2249	10.74	-5.14	-65.1	0.175	1003	0.3058	-0.3492
222	3591	0.195	2254	37.79	-28.81	-106.4	0.024	993	0.3071	-0.5680
219	3605	0.095	2256	42.19	-28.63	-93.9	0.017	993	0.3080	-0.5003
231	3595	0.442	2247	26.90	-27.61	-141.7	0.044	982	0.3084	-0.7615
996	3612	0.905	2252	5.78	-1.85	-42.4	0.165	482	0.3091	-0.2271
378	3609	0.257	2247	34.07	-15.39	-58.2	0.032	1184	0.3096	-0.3126
380	3633	0.290	2258	32.66	-14.35	-56.9	0.030	1188	0.3101	-0.3026
293	3641	0.443	2259	26.81	-17.81	-87.9	0.044	989	0.3107	-0.4673
382	3612	0.438	2241	26.43	-14.85	-74.8	0.049	1180	0.3107	-0.4041
364	3623	0.150	2244	38.47	-15.85	-52.4	0.017	1204	0.3112	-0.2822
351	3672	0.279	2265	34.10	-20.61	-77.0	0.031	984	0.3125	-0.4072
220	3657	0.108	2252	41.62	-28.81	-95.2	0.018	995	0.3130	-0.5095
917	3656	0.903	2243	6.27	-2.59	-56.5	0.266	844	0.3142	-0.3046
349	3661	0.154	2246	39.57	-16.91	-52.3	0.019	991	0.3142	-0.2815
312	3684	0.452	2246	26.41	-16.23	-81.9	0.046	990	0.3161	-0.4403
801	3701	0.264	2255	34.95	-19.41	-72.6	0.025	954	0.3164	-0.3876
800	3709	0.272	2252	34.61	-19.73	-74.6	0.026	955	0.3174	-0.3989
296	3693	0.139	2242	41.28	-19.99	-57.8	0.018	829	0.3175	-0.3122
1391	8562	0.808	5197	10.61	-28.39	-299.2	0.099	468	0.3176	-0.3006
962	3703	0.123	2243	44.60	-20.30	-49.7	0.026	491	0.3182	-0.2683
388	3749	0.468	2248	26.21	-16.93	-84.1	0.056	834	0.3215	-0.4515
986	3808	0.675	2241	17.24	-9.55	-71.3	0.048	478	0.3275	-0.3855
294	3851	0.335	2258	31.62	-26.19	-107.3	0.032	977	0.3288	-0.5712
389	3879	0.328	2254	32.61	-29.61	-115.6	0.041	825	0.3317	-0.6174
744	4541	0.490	2617	25.18	-33.12	-175.0	0.057	848	0.3345	-0.6933
751	3534	0.530	2025	23.40	-16.50	-96.4	0.061	828	0.3364	-0.6376
761	3950	0.685	2248	16.37	-13.02	-109.5	0.092	745	0.3387	-0.5877
390	3953	0.218	2249	37.68	-29.79	-96.4	0.033	825	0.3388	-0.5174
750	3561	0.561	2026	21.98	-15.04	-93.8	0.067	826	0.3388	-0.6201
966	3986	0.452	2250	28.44	-27.50	-111.5	0.031	454	0.3415	-0.5975
772	3610	0.547	2023	22.63	-18.32	-113.6	0.064	833	0.3439	-0.7529
749	3620	0.567	2024	21.68	-17.15	-108.9	0.068	825	0.3447	-0.7216
754	3666	0.623	2047	19.19	-14.23	-102.2	0.079	806	0.3452	-0.6617
762	4032	0.727	2251	14.43	-12.40	-119.1	0.107	743	0.3453	-0.6377
1385	8016	0.897	4459	6.21	-16.86	-360.9	0.177	539	0.3465	-0.4925
812	4051	0.684	2249	16.46	-11.36	-95.6	0.083	733	0.3472	-0.5129
763	4054	0.713	2249	15.06	-12.52	-114.6	0.101	742	0.3475	-0.6150
786	4473	0.988	2478	1.20	-0.85	-99.6	0.547	274	0.3480	-0.4403
748	3628	0.575	2000	21.36	-16.10	-103.4	0.069	828	0.3496	-0.7011
753	3714	0.632	2047	18.79	-14.71	-107.9	0.080	796	0.3497	-0.6989
747	3646	0.576	2006	21.30	-16.04	-103.1	0.069	827	0.3503	-0.6952
752	3733	0.633	2046	18.73	-14.37	-105.7	0.081	796	0.3517	-0.6850

TEST #	Q gpm	α_{avg}	N rpm	ρ lbm/ft^3	Δp psi	H_o ft	x_{ups}	p psi	ϕ	ψ'
813	4114	0.738	2254	13.92	-10.29	-103.1	0.101	731	0.3518	-0.5507
811	4104	0.659	2244	17.54	-12.25	-95.8	0.079	784	0.3525	-0.5160
810	4125	0.631	2244	18.76	-15.33	-112.3	0.074	833	0.3544	-0.6052
352	3733	0.285	2024	33.83	-30.49	-117.3	0.033	978	0.3555	-0.7768
814	4159	0.767	2252	12.55	-9.20	-102.6	0.114	730	0.3560	-0.5491
1433	4170	0.387	2253	31.65	-34.74	-114.0	0.033	457	0.3567	-0.6092
757	3997	0.650	2158	17.96	-17.50	-134.4	0.085	789	0.3570	-0.7828
802	4206	0.266	2267	34.87	-36.93	-136.9	0.030	945	0.3576	-0.7225
745	4519	0.491	2433	25.08	-35.36	-187.8	0.058	864	0.3580	-0.8608
816	4178	0.814	2249	10.32	-8.00	-108.6	0.133	636	0.3581	-0.5825
815	4194	0.815	2252	10.28	-8.04	-109.5	0.132	636	0.3590	-0.5860
805	4231	0.573	2245	21.41	-21.92	-140.0	0.062	828	0.3633	-0.7535
809	4231	0.573	2245	21.41	-21.92	-140.0	0.062	828	0.3633	-0.7535
1412	4514	0.645	2379	18.21	-19.01	-138.7	0.075	771	0.3657	-0.6648
766	4362	0.754	2291	13.15	-13.43	-141.1	0.115	696	0.3670	-0.7294
746	4320	0.420	2249	28.14	-39.95	-189.5	0.050	914	0.3703	-1.0164
808	4370	0.546	2238	22.64	-23.67	-142.5	0.057	835	0.3764	-0.7718
807	4441	0.500	2242	24.68	-34.43	-190.3	0.052	867	0.3818	-1.0272
1387	8895	0.918	4466	5.07	-19.07	-497.2	0.191	461	0.3839	-0.6763
1389	8964	0.925	4462	4.75	-18.96	-530.0	0.202	458	0.3873	-0.7224
1435	4545	0.404	2257	30.85	-43.44	-141.0	0.039	449	0.3882	-0.7509
806	4595	0.472	2247	25.89	-41.03	-214.5	0.050	885	0.3942	-1.1527
1388	9142	0.931	4458	4.45	-20.55	-619.8	0.216	461	0.3953	-0.8462
770	4807	0.808	2338	10.59	-15.32	-201.5	0.135	629	0.3963	-1.0002
299	4718	0.473	2286	25.54	-42.03	-215.5	0.052	970	0.3978	-1.1191
1413	4955	0.678	2378	16.69	-26.42	-212.7	0.086	776	0.4017	-1.0204
1386	9447	0.935	4464	4.26	-20.63	-651.7	0.222	441	0.4079	-0.8874
803	4471	0.397	2095	29.13	-50.28	-228.3	0.044	917	0.4113	-1.4115
1434	4965	0.551	2261	23.46	-40.30	-192.6	0.045	459	0.4233	-1.0224
804	4324	0.366	1966	30.56	-50.49	-217.7	0.041	912	0.4239	-1.5280
965	4234	0.252	1922	38.39	-51.81	-138.8	0.043	453	0.4246	-1.0193
817	4975	0.981	2248	1.67	-2.29	-195.1	0.441	301	0.4266	-1.0473
819	5131	0.990	2250	1.19	-1.96	-234.0	0.577	300	0.4396	-1.2544
964	4400	0.306	1921	35.66	-56.30	-160.3	0.048	454	0.4415	-1.1783
963	4769	0.417	2082	30.14	-53.63	-185.8	0.052	452	0.4416	-1.1629
1410	4929	0.817	2145	10.14	-13.57	-180.7	0.099	539	0.4429	-1.0656
820	5290	0.993	2249	1.02	-2.05	-289.2	0.669	304	0.4534	-1.5515
821	5404	0.993	2251	1.01	-2.15	-304.8	0.677	302	0.4628	-1.6324
1124	4010	0.991	1568	1.47	-1.50	-143.3	0.743	482	0.4929	-1.5817
1125	4360	0.992	1568	1.44	-1.93	-188.9	0.756	483	0.5359	-2.0851
1126	4319	0.992	1485	1.45	-2.00	-196.0	0.754	483	0.5606	-2.4116
913	5081	0.807	1574	10.67	-23.33	-304.8	0.147	829	0.6223	-3.3380
915	5116	0.953	1565	4.02	-10.55	-373.0	0.439	843	0.6302	-4.1325
914	5204	0.907	1567	6.08	-15.75	-366.4	0.275	828	0.6401	-4.0492
910	4255	0.684	1249	16.31	-28.33	-240.1	0.085	826	0.6566	-4.1753

TEST #	Q gpm	α_{avg}	N rpm	ρ lbm/ft^3	Δp psi	H_o ft	x_{ups}	p psi	ϕ	ψ'
909	4240	0.681	1212	16.48	-30.19	-253.6	0.084	825	0.6743	-4.6841
1409	4810	0.887	1326	6.68	-12.12	-252.2	0.151	521	0.6993	-3.8921
1393	4624	0.504	1270	24.20	-62.91	-350.3	0.060	969	0.7018	-5.8939
1408	11544	0.983	3085	1.73	-25.41	-2048.6	0.484	390	0.7213	-5.8407
908	4741	0.572	1246	21.52	-62.11	-390.3	0.063	798	0.7335	-6.8220
1403	12613	0.980	2693	1.60	-27.75	-2394.4	0.367	257	0.9028	-8.9584
1406	11385	0.984	2019	1.73	-30.46	-2467.3	0.499	406	1.0870	-16.4234
1407	12182	0.960	2049	2.90	-50.59	-2356.8	0.290	382	1.1461	-15.2315
1404	11771	0.981	1830	1.65	-28.23	-2368.1	0.395	290	1.2399	-19.1873
1405	12426	0.982	1831	1.52	-28.96	-2618.2	0.383	262	1.3082	-21.1900

B.3. Second-Quadrant, Single-Phase Data

TEST #	Q gpm	α_{avg}	N rpm	ρ lbm/ft^3	Δp psi	H_o ft	x_{ups}	p psi	ϕ	ψ'
432	-249	0.000	4463	61.08	153.58	363.1	0.000	111	-0.0107	0.4947
397	-183	0.000	2244	61.07	38.37	91.5	0.000	48	-0.0157	0.4928
436	-870	0.000	2247	46.54	38.65	120.6	0.000	967	-0.0746	0.6482
430	-894	0.000	2242	61.64	48.96	115.4	0.000	54	-0.0768	0.6230
431	-1818	0.000	2236	61.42	77.80	183.5	0.000	76	-0.1567	0.9958
1468	-1800	0.000	1787	47.47	45.59	139.4	0.000	958	-0.1942	1.1841
1469	-1823	0.000	1803	47.36	45.89	140.6	0.000	979	-0.1949	1.1734
495	-869	0.000	807	48.35	10.08	31.1	0.000	835	-0.2076	1.2955
494	-1697	0.000	787	48.15	29.83	90.3	0.000	826	-0.4155	3.9576
496	-1945	0.000	786	45.60	36.44	116.2	0.000	1132	-0.4770	5.1020
487	-1962	0.000	776	57.13	47.65	121.0	0.000	118	-0.4873	5.4510
488	-1970	0.000	777	52.45	43.52	120.6	0.000	390	-0.4887	5.4194
489	-1981	0.000	781	47.26	38.60	118.8	0.000	926	-0.4888	5.2836
486	-1963	0.000	772	60.81	51.31	122.5	0.000	15	-0.4902	5.5749
493	-2265	0.000	767	48.66	51.52	153.7	0.000	813	-0.5691	7.0881
1509	-2831	0.000	763	47.31	75.49	230.9	0.000	959	-0.7151	10.7616
492	-2855	0.000	739	48.41	79.81	238.6	0.000	804	-0.7447	11.8538
524	-802	1.000	2249	2.24	2.56	166.8	1.000	996	-0.0687	0.8948

B.4. Second-Quadrant, Two-Phase Data

TEST #	Q gpm	α_{avg}	N rpm	ρ lbm/ft^3	Δp psi	H_o ft	x_{ups}	p psi	ϕ	ψ'
1478	-110	0.275	4485	35.24	89.91	368.4	0.184	844	-0.0047	0.4969
1480	-490	0.862	4479	8.15	63.81	1127.6	0.190	823	-0.0211	1.5251
1479	-503	0.851	4478	8.64	65.04	1084.9	0.191	840	-0.0217	1.4681
1476	-443	0.505	3608	24.12	52.44	313.6	0.077	979	-0.0237	0.6537
1475	-490	0.560	3609	21.66	51.37	342.2	0.087	978	-0.0262	0.7129
1474	-496	0.560	3598	21.69	53.37	355.0	0.089	978	-0.0266	0.7440
1473	-515	0.593	3600	20.23	50.76	362.0	0.104	981	-0.0275	0.7578
1477	-1034	0.840	4492	9.14	62.03	977.0	0.158	827	-0.0444	1.3138
417	-735	0.354	2243	30.72	29.50	138.6	0.045	992	-0.0631	0.7476
522	-990	0.108	2231	41.65	40.96	141.9	0.053	984	-0.0855	0.7737
418	-1020	0.816	2248	10.32	18.21	254.3	0.192	984	-0.0874	1.3654
523	-1076	0.444	2236	26.80	32.09	172.3	0.095	984	-0.0928	0.9351
437	-1170	0.367	2242	30.19	37.58	178.8	0.070	976	-0.1006	0.9653
538	-2062	0.260	2942	35.25	90.48	362.5	0.047	910	-0.1351	1.1364
506	-1038	0.411	1290	28.21	16.22	83.1	0.045	996	-0.1550	1.3551
507	-1272	0.431	1547	27.35	22.59	118.9	0.047	989	-0.1584	1.3479
505	-926	0.457	1120	26.19	12.27	67.9	0.047	991	-0.1593	1.4690
508	-2519	0.469	2832	25.75	79.43	437.2	0.060	960	-0.1715	1.4790
439	-2267	0.205	2149	36.35	69.82	271.8	0.041	1159	-0.2034	1.5972
438	-2322	0.215	2147	36.99	75.02	284.8	0.042	962	-0.2084	1.6765
1471	-2247	0.319	1804	32.35	57.76	252.6	0.051	988	-0.2401	2.1059
540	-3261	0.312	1729	32.97	99.25	414.4	0.049	902	-0.3635	3.7611
539	-3342	0.334	1756	31.97	97.94	421.6	0.051	902	-0.3668	3.7095
420	-1850	0.437	886	27.06	26.66	140.6	0.046	994	-0.4024	4.8606
1472	-3098	0.328	1013	32.02	76.11	331.0	0.044	971	-0.5895	8.7521
419	-3694	0.490	1059	24.80	79.66	447.3	0.062	963	-0.6724	10.8224

B.5. Third-Quadrant, Single-Phase Data

TEST #	Q gpm	α_{avg}	N rpm	ρ lbm/ft^3	Δp psi	H_o ft	x_{ups}	p psi	ϕ	ψ'
1505	-1297	0.000	-4017	48.42	28.63	86.2	0.000	845	0.0622	0.1449
395	-1806	0.000	-4499	60.94	56.36	134.1	0.000	61	0.0774	0.1798
393	-906	0.000	-2244	61.05	13.30	32.3	0.000	35	0.0778	0.1742
1506	-1821	0.000	-4027	48.29	36.31	109.4	0.000	834	0.0872	0.1830
1507	-2243	0.000	-4032	48.22	40.28	121.4	0.000	889	0.1072	0.2026
396	-2698	0.000	-4504	60.90	68.20	162.2	0.000	74	0.1155	0.2170
1508	-2615	0.000	-4042	48.18	44.79	135.0	0.000	876	0.1247	0.2242
1488	-2697	0.000	-3777	60.94	57.34	136.5	0.000	206	0.1376	0.2596
1504	-2920	0.000	-4052	48.16	52.24	157.4	0.000	867	0.1389	0.2601
1498	-3169	0.000	-4398	51.81	66.87	186.9	0.000	462	0.1389	0.2622
422	-2391	0.000	-3148	47.32	34.14	105.1	0.000	979	0.1464	0.2877
1486	-3190	0.000	-4084	60.98	80.26	190.5	0.000	202	0.1506	0.3100
394	-1771	0.000	-2251	61.05	24.09	57.8	0.000	45	0.1517	0.3093
1503	-3223	0.000	-4061	48.10	63.23	190.5	0.000	853	0.1530	0.3134
1490	-1958	0.000	-2324	60.89	29.98	71.9	0.000	197	0.1624	0.3612
1491	-1554	0.000	-1807	60.90	18.73	45.3	0.000	299	0.1657	0.3763
1487	-2958	0.000	-3440	60.97	68.77	163.5	0.000	214	0.1658	0.3748
1489	-2365	0.000	-2740	60.92	43.72	104.4	0.000	211	0.1664	0.3771
1494	-2061	0.000	-2380	57.53	31.06	78.8	0.000	186	0.1669	0.3777
1496	-1507	0.000	-1737	53.28	15.27	42.3	0.000	423	0.1672	0.3808
402	-3212	0.000	-3597	45.08	59.94	192.7	0.000	1222	0.1721	0.4042
401	-3215	0.000	-3596	45.46	60.35	192.4	0.000	1176	0.1723	0.4037
421	-2392	0.000	-2243	47.31	35.74	110.0	0.000	976	0.2055	0.5932
511	-544	0.000	-428	45.33	1.59	6.1	0.000	1200	0.2450	0.9013
513	-541	0.000	-406	44.98	1.45	5.7	0.000	1211	0.2566	0.9353
512	-426	0.000	-282	45.06	0.92	4.0	0.000	1211	0.2909	1.3548
518	-2315	1.000	-3148	2.24	1.72	114.7	1.000	998	0.1418	0.3140
428	-2351	1.000	-2239	2.22	1.75	117.0	1.000	993	0.2024	0.6333

B.6. Third-Quadrant, Two-Phase Data

TEST #	Q gpm	α_{avg}	N rpm	ρ lbm/ft^3	Δp psi	H_o ft	x_{ups}	p psi	ϕ	ψ'
412	-395	0.503	-2246	24.16	6.59	40.0	0.077	1000	0.0339	0.2153
411	-843	0.391	-4497	29.11	26.67	132.1	0.053	990	0.0361	0.1773
521	-1150	0.453	-4710	26.37	30.94	168.7	0.088	991	0.0470	0.2064
425	-2736	0.471	-6701	25.61	62.88	346.3	0.052	967	0.0787	0.2092
427	-1282	0.427	-2240	27.49	8.28	43.5	0.042	1002	0.1103	0.2352
424	-2678	0.472	-4483	25.59	30.71	169.2	0.049	978	0.1152	0.2284
409	-4273	0.490	-6739	24.81	76.03	419.6	0.062	960	0.1222	0.2507
415	-2504	0.805	-3145	10.82	9.83	130.2	0.179	991	0.1535	0.3571
543	-3945	0.653	-4900	17.66	37.61	297.7	0.096	884	0.1552	0.3365
544	-4409	0.756	-5469	13.03	37.89	408.7	0.132	828	0.1554	0.3708
414	-2540	0.436	-3142	27.13	23.28	120.9	0.046	988	0.1558	0.3324
542	-3651	0.401	-4490	29.03	53.09	249.1	0.052	892	0.1567	0.3353
413	-2641	0.184	-3143	38.25	32.16	116.1	0.022	984	0.1619	0.3190
408	-4403	0.464	-4501	25.91	67.88	355.6	0.058	968	0.1886	0.4763
558	-4405	0.802	-4187	10.92	27.62	351.9	0.115	525	0.2028	0.5447
406	-2437	0.800	-2226	11.07	8.58	111.0	0.171	987	0.2110	0.6081
426	-2493	0.605	-2244	19.67	15.89	115.1	0.076	990	0.2141	0.6202
517	-2484	0.955	-2233	4.22	3.45	117.2	0.554	995	0.2144	0.6377
405	-2565	0.438	-2238	27.09	23.81	123.9	0.046	974	0.2209	0.6711
404	-2680	0.286	-2242	33.77	32.29	133.3	0.030	983	0.2304	0.7196
403	-2708	0.130	-2247	40.62	36.47	124.0	0.019	990	0.2323	0.6364
423	-2737	0.219	-2247	36.79	34.99	131.7	0.024	978	0.2348	0.7076
541	-4068	0.374	-2168	30.19	79.21	355.0	0.052	896	0.3617	2.0493
407	-4254	0.442	-2246	26.92	77.03	390.9	0.055	960	0.3651	2.1025
503	-2931	0.448	-1133	26.65	38.35	202.4	0.052	977	0.4986	4.2792
504	-2961	0.455	-1132	26.33	38.91	208.0	0.053	980	0.5042	4.4048

APPENDIX C

CORRELATION DATA

Two-phase data from Appendix B are here presented in the form of head-loss ratios (H^*) and head ratios (ψ'_{tp}/ψ'_{sp}). Only those test points with flow coefficients within the range of the single-phase flow data are included here; no attempt was made to extrapolate the single-phase performance beyond that which was tested by Combustion Engineering. The single-phase head coefficients were calculated from the least-squares polynomial fits (see Chapter 3), and calculaton of the theoretical head coefficients was discussed in Chapters 2 and 3. System pressures (average) and void fractions (both upstream and average) are included for correlation purposes.

C.1. First-Quadrant Data

TEST #	ϕ_{tp}	ψ'_{tp}	ψ'_{sp}	ψ'_{th}	H^*	ψ'_{tp}/ψ'_{sp}	α_{ups}	α_{avg}	p psi
289	0.007	0.471	0.468	0.573	0.976	1.005	0.565	0.283	1018
287	0.012	0.475	0.467	0.568	0.919	1.017	0.421	0.211	1013
1420	0.015	0.179	0.466	0.565	3.911	0.384	0.386	0.533	989
920	0.016	0.213	0.466	0.565	3.570	0.458	0.817	0.844	850
921	0.018	0.248	0.466	0.563	3.243	0.533	0.472	0.528	1016
1417	0.020	0.231	0.465	0.561	3.435	0.497	0.478	0.589	987
276	0.038	0.163	0.456	0.544	4.348	0.357	0.816	0.821	869
922	0.040	0.262	0.454	0.541	3.217	0.576	0.425	0.431	1023
277	0.044	0.182	0.451	0.537	4.150	0.402	0.852	0.855	856
286	0.049	0.293	0.448	0.533	2.836	0.653	0.411	0.362	1029
285	0.050	0.324	0.447	0.532	2.454	0.725	0.385	0.342	1032
275	0.054	0.149	0.444	0.528	4.515	0.335	0.813	0.820	846
229	0.059	0.246	0.439	0.523	3.305	0.561	0.488	0.464	1004
362	0.063	0.214	0.436	0.519	3.656	0.491	0.399	0.417	1019

TEST #	ϕ_{tp}	ψ'_{tp}	ψ'_{sp}	ψ'_{th}	H^*	ψ'_{tp}/ψ'_{sp}	α_{ups}	α_{avg}	p psi
284	0.074	0.234	0.424	0.509	3.260	0.551	0.369	0.340	1007
271	0.075	0.173	0.423	0.507	3.952	0.409	0.795	0.785	869
228	0.082	0.183	0.415	0.501	3.699	0.441	0.485	0.463	1001
217	0.088	0.203	0.407	0.495	3.335	0.497	0.380	0.343	920
888	0.090	0.331	0.405	0.493	1.837	0.817	0.253	0.177	1021
281	0.091	0.213	0.403	0.492	3.136	0.529	0.501	0.468	1004
363	0.095	0.266	0.398	0.488	2.455	0.670	0.389	0.417	1008
226	0.096	0.217	0.397	0.488	2.989	0.546	0.481	0.458	1001
237	0.096	0.211	0.396	0.487	3.034	0.534	0.514	0.503	1000
270	0.097	0.147	0.396	0.487	3.738	0.371	0.798	0.794	856
239	0.104	0.205	0.384	0.479	2.896	0.533	0.471	0.459	996
339	0.105	0.212	0.384	0.479	2.811	0.552	0.426	0.418	1002
225	0.107	0.230	0.380	0.476	2.557	0.605	0.429	0.416	1010
334	0.109	0.241	0.377	0.474	2.392	0.640	0.432	0.347	1036
283	0.110	0.152	0.376	0.474	3.284	0.404	0.456	0.445	998
273	0.112	0.093	0.373	0.472	3.832	0.249	0.811	0.821	846
242	0.113	0.209	0.371	0.471	2.628	0.562	0.427	0.411	1000
571	0.122	0.285	0.356	0.462	1.666	0.801	0.235	0.143	1158
359	0.123	0.221	0.354	0.461	2.240	0.625	0.415	0.358	1029
361	0.125	0.220	0.350	0.459	2.197	0.629	0.404	0.379	1023
338	0.125	0.222	0.351	0.459	2.190	0.633	0.436	0.417	1012
719	0.126	0.145	0.350	0.459	2.885	0.415	0.195	0.187	968
720	0.128	0.166	0.346	0.456	2.623	0.480	0.175	0.165	969
279	0.130	0.276	0.343	0.455	1.597	0.804	0.230	0.157	1020
235	0.134	0.164	0.335	0.451	2.474	0.491	0.458	0.450	1007
988	0.136	0.061	0.331	0.449	3.284	0.186	0.613	0.617	487
243	0.136	0.190	0.332	0.449	2.205	0.574	0.366	0.343	996
223	0.137	0.318	0.328	0.447	1.087	0.968	0.137	0.069	1028
881	0.138	0.123	0.327	0.447	2.710	0.375	0.218	0.144	472
572	0.138	0.354	0.326	0.446	0.768	1.085	0.041	0.021	1157
967	0.139	0.099	0.325	0.446	2.875	0.304	0.371	0.342	487
264	0.139	0.048	0.325	0.446	3.298	0.148	0.788	0.785	481
959	0.140	0.094	0.324	0.445	2.897	0.289	0.434	0.462	1004
1122	0.140	0.234	0.324	0.445	1.737	0.724	0.989	0.991	482
377	0.140	0.326	0.324	0.445	0.979	1.008	0.102	0.051	1222
234	0.143	0.179	0.318	0.442	2.121	0.562	0.416	0.406	1010
278	0.144	0.234	0.316	0.441	1.656	0.740	0.234	0.182	1007
990	0.145	0.115	0.312	0.440	2.548	0.369	0.197	0.132	484
1115	0.145	0.246	0.313	0.440	1.525	0.787	0.187	0.126	955
269	0.145	0.090	0.313	0.440	2.760	0.288	0.795	0.795	851
1116	0.146	0.257	0.312	0.439	1.427	0.825	0.187	0.126	970
354	0.146	0.215	0.312	0.439	1.758	0.690	0.947	0.951	1001
355	0.146	0.174	0.311	0.439	2.073	0.559	0.908	0.913	1002
991	0.147	0.111	0.310	0.438	2.552	0.357	0.208	0.144	486

TEST #	ϕ_{tp}	ψ'_{tp}	ψ'_{sp}	ψ'_{th}	H^*	ψ'_{tp}/ψ'_{sp}	α_{ups}	α_{avg}	p psi
1114	0.147	0.232	0.310	0.438	1.605	0.749	0.203	0.146	975
721	0.147	0.190	0.309	0.438	1.928	0.614	0.297	0.288	972
381	0.147	0.279	0.309	0.438	1.232	0.903	0.274	0.245	1210
992	0.148	0.103	0.307	0.437	2.572	0.336	0.216	0.157	486
911	0.148	0.086	0.306	0.437	2.688	0.282	0.640	0.643	852
1113	0.148	0.213	0.307	0.437	1.720	0.694	0.219	0.169	951
347	0.148	0.122	0.307	0.437	2.421	0.398	0.801	0.807	1013
346	0.148	0.120	0.308	0.437	2.450	0.390	0.633	0.641	1004
216	0.148	0.206	0.308	0.437	1.784	0.669	0.224	0.183	1019
387	0.149	0.106	0.305	0.436	2.520	0.346	0.794	0.801	843
215	0.149	0.292	0.304	0.436	1.089	0.962	0.112	0.056	1024
333	0.150	0.148	0.304	0.435	2.177	0.489	0.432	0.402	1013
233	0.150	0.171	0.304	0.436	2.011	0.562	0.387	0.376	1010
989	0.151	0.057	0.301	0.434	2.839	0.188	0.650	0.656	477
350	0.151	0.281	0.301	0.434	1.151	0.933	0.176	0.123	1020
313	0.151	0.149	0.300	0.434	2.128	0.497	0.420	0.421	994
379	0.152	0.264	0.298	0.433	1.250	0.887	0.196	0.157	1225
994	0.153	0.080	0.296	0.432	2.586	0.270	0.901	0.904	480
918	0.153	0.191	0.296	0.432	1.766	0.647	0.951	0.953	846
232	0.154	0.184	0.294	0.431	1.801	0.626	0.317	0.296	1004
995	0.155	0.130	0.292	0.430	2.171	0.444	0.948	0.951	479
1112	0.155	0.185	0.292	0.430	1.771	0.635	0.266	0.240	961
961	0.156	0.172	0.291	0.430	1.854	0.592	0.423	0.420	1113
344	0.159	0.119	0.284	0.427	2.159	0.419	0.447	0.452	999
993	0.160	0.049	0.282	0.426	2.624	0.174	0.817	0.822	474
332	0.162	0.140	0.277	0.424	1.937	0.504	0.427	0.417	1003
224	0.170	0.162	0.260	0.416	1.626	0.622	0.366	0.364	996
960	0.171	0.130	0.256	0.415	1.787	0.510	0.496	0.498	1178
987	0.172	0.041	0.255	0.414	2.341	0.161	0.688	0.693	479
238	0.181	0.066	0.232	0.405	1.959	0.283	0.497	0.506	995
919	0.183	0.073	0.226	0.403	1.863	0.323	0.801	0.805	846
903	0.191	0.132	0.205	0.396	1.384	0.643	0.248	0.245	1000
240	0.193	0.054	0.200	0.394	1.757	0.269	0.442	0.452	987
742	0.195	0.066	0.194	0.392	1.653	0.338	0.503	0.503	866
360	0.200	0.083	0.182	0.387	1.461	0.456	0.411	0.426	989
569	0.200	0.198	0.180	0.387	0.910	1.103	0.052	0.056	1217
740	0.202	0.072	0.174	0.385	1.480	0.416	0.449	0.450	902
739	0.208	0.050	0.156	0.379	1.479	0.317	0.394	0.398	937
241	0.209	0.044	0.155	0.379	1.497	0.285	0.408	0.420	992
738	0.211	0.074	0.149	0.377	1.327	0.500	0.340	0.343	934
958	0.212	0.044	0.144	0.375	1.435	0.303	0.794	0.799	996
726	0.215	0.038	0.135	0.372	1.413	0.278	0.361	0.365	947
280	0.215	0.017	0.135	0.372	1.495	0.128	0.429	0.433	994
274	0.220	-0.145	0.119	0.367	2.065	-1.219	0.811	0.820	849

TEST #	ϕ_{tp}	ψ'_{tp}	ψ'_{sp}	ψ'_{th}	H^*	ψ'_{tp}/ψ'_{sp}	α_{ups}	α_{avg}	p psi
331	0.220	0.022	0.120	0.367	1.393	0.186	0.396	0.424	980
292	0.220	0.060	0.121	0.368	1.248	0.497	0.422	0.438	993
330	0.222	0.016	0.115	0.366	1.396	0.138	0.404	0.432	956
901	0.223	0.062	0.110	0.365	1.192	0.559	0.231	0.245	990
902	0.226	0.031	0.099	0.362	1.259	0.317	0.359	0.374	988
904	0.227	0.009	0.097	0.361	1.334	0.092	0.667	0.674	1002
1416	0.228	0.044	0.093	0.360	1.185	0.473	0.225	0.250	955
1415	0.229	0.029	0.091	0.359	1.234	0.316	0.260	0.284	949
900	0.231	0.045	0.084	0.357	1.139	0.545	0.167	0.184	995
314	0.234	-0.023	0.075	0.355	1.351	-0.305	0.424	0.455	986
265	0.237	-0.136	0.062	0.351	1.687	-2.179	0.876	0.876	522
737	0.239	-0.015	0.056	0.349	1.241	-0.270	0.414	0.420	938
384	0.240	-0.024	0.053	0.349	1.261	-0.458	0.716	0.725	850
773	0.260	-0.069	-0.026	0.329	1.122	2.669	0.263	0.276	947
263	0.269	-0.212	-0.061	0.320	1.397	3.480	0.770	0.772	481
1123	0.270	-0.055	-0.065	0.320	0.974	0.846	0.988	0.990	482
297	0.272	-0.235	-0.076	0.317	1.404	3.085	0.155	0.198	826
266	0.277	-0.354	-0.098	0.312	1.625	3.623	0.946	0.940	482
570	0.286	-0.124	-0.138	0.304	0.968	0.899	0.064	0.120	1205
1394	0.287	-0.275	-0.142	0.303	1.300	1.938	0.435	0.482	936
1395	0.290	-0.283	-0.157	0.300	1.274	1.796	0.418	0.468	917
353	0.290	-0.269	-0.157	0.300	1.244	1.709	0.947	0.951	1001
230	0.293	-0.383	-0.174	0.297	1.443	2.200	0.428	0.449	978
386	0.296	-0.209	-0.188	0.294	1.043	1.110	0.792	0.800	843
356	0.296	-0.296	-0.185	0.295	1.232	1.601	0.906	0.911	997
1396	0.300	-0.341	-0.205	0.291	1.275	1.665	0.414	0.466	916
1414	0.302	-0.332	-0.218	0.288	1.226	1.524	0.674	0.690	767
383	0.302	-0.317	-0.215	0.289	1.201	1.472	0.786	0.794	1195
221	0.302	-0.556	-0.215	0.289	1.675	2.579	0.165	0.179	991
912	0.303	-0.289	-0.220	0.288	1.135	1.310	0.659	0.669	835
345	0.303	-0.344	-0.225	0.287	1.234	1.533	0.655	0.664	999
348	0.306	-0.349	-0.237	0.285	1.215	1.474	0.799	0.807	1003
222	0.307	-0.568	-0.243	0.284	1.616	2.333	0.180	0.195	993
231	0.308	-0.762	-0.251	0.282	1.958	3.038	0.415	0.442	982
219	0.308	-0.500	-0.249	0.283	1.474	2.012	0.074	0.095	993
996	0.309	-0.227	-0.255	0.282	0.949	0.892	0.901	0.905	482
380	0.310	-0.303	-0.260	0.281	1.079	1.164	0.253	0.290	1188
378	0.310	-0.313	-0.257	0.281	1.103	1.216	0.214	0.257	1184
382	0.311	-0.404	-0.263	0.280	1.260	1.537	0.409	0.438	1180
364	0.311	-0.282	-0.266	0.280	1.030	1.061	0.102	0.150	1204
293	0.311	-0.467	-0.263	0.280	1.376	1.776	0.407	0.443	989
351	0.312	-0.407	-0.273	0.278	1.244	1.493	0.220	0.279	984
220	0.313	-0.509	-0.276	0.278	1.422	1.848	0.083	0.108	995
917	0.314	-0.305	-0.282	0.277	1.040	1.079	0.900	0.903	844

TEST #	ϕ_{tp}	ψ'_{tp}	ψ'_{sp}	ψ'_{th}	H^*	ψ'_{tp}/ψ'_{sp}	α_{ups}	α_{avg}	p psi
349	0.314	-0.282	-0.282	0.277	0.998	0.997	0.092	0.154	991
312	0.316	-0.440	-0.293	0.275	1.259	1.502	0.424	0.452	990
801	0.316	-0.388	-0.295	0.275	1.163	1.316	0.223	0.264	954
800	0.317	-0.399	-0.301	0.274	1.171	1 327	0.230	0.272	955
1391	0.318	-0.301	-0.301	0.273	0.999	0.998	0.781	0.808	468
962	0.318	-0.268	-0.305	0.273	0.937	0.880	0.018	0.123	491
296	0.318	-0.312	-0.301	0.273	1.020	1.037	0.059	0.139	829
388	0.321	-0.451	-0.324	0.270	1.215	1.395	0.430	0.468	834
986	0.328	-0.385	-0.359	0.264	1.042	1.073	0.655	0.675	478
294	0.329	-0.571	-0.367	0.263	1.325	1.557	0.276	0.335	977
389	0.332	-0.617	-0.385	0.260	1.361	1.604	0.253	0.328	825
744	0.334	-0.693	-0.402	0.257	1.442	1.725	0.450	0.490	848
751	0.336	-0.638	-0.414	0.255	1.334	1.540	0.510	0.530	828
761	0.339	-0.588	-0.429	0.253	1.233	1.370	0.674	0.685	745
750	0.339	-0.620	-0.430	0.253	1.279	1.444	0.544	0.561	826
390	0.339	-0.517	-0.430	0.253	1.129	1.204	0.122	0.218	825
966	0.341	-0.598	-0.447	0.250	1.216	1.337	0.348	0.452	454
772	0.344	-0.753	-0.463	0.248	1.408	1.626	0.539	0.547	833
762	0.345	-0.638	-0.472	0.247	1.231	1.351	0.718	0.727	743
754	0.345	-0.662	-0.471	0.247	1.265	1.404	0.609	0.623	806
749	0.345	-0.722	-0.468	0.247	1.354	1.541	0.550	0.567	825
1385	0.347	-0.493	-0.480	0.245	1.017	1.025	0.891	0.897	539
812	0.347	-0.513	-0.485	0.245	1.038	1.058	0.676	0.684	733
763	0.347	-0.615	-0.487	0.245	1.176	1.264	0.703	0.713	742
786	0.348	-0.440	-0.490	0.244	0.932	0.899	0.987	0.988	274
753	0.350	-0.699	-0.502	0.242	1.265	1.393	0.618	0.632	796
748	0.350	-0.701	-0.501	0.243	1.269	1.399	0.557	0.575	828
747	0.350	-0.695	-0.506	0.242	1.253	1.374	0.558	0.576	827
813	0.352	-0.551	-0.516	0.240	1.045	1.066	0.732	0.738	731
752	0.352	-0.685	-0.516	0.240	1.224	1.329	0.619	0.633	796
811	0.353	-0.516	-0.521	0.240	0.993	0.990	0.648	0.659	784
810	0.354	-0.605	-0.534	0.238	1.092	1.133	0.618	0.631	833
352	0.355	-0.777	-0.542	0.237	1.302	1.433	0.214	0.285	978
814	0.356	-0.549	-0.545	0.236	1.005	1.007	0.762	0.767	730
1433	0.357	-0.609	-0.551	0.236	1.074	1.106	0.217	0.387	457
757	0.357	-0.783	-0.553	0.235	1.292	1.416	0.635	0.650	789
816	0.358	-0.583	-0.561	0.234	1.028	1.039	0.810	0.814	636
745	0.358	-0.861	-0.560	0.234	1.378	1.537	0.448	0.491	864
802	0.358	-0.723	-0.557	0.235	1.209	1.297	0.194	0.266	945
815	0.359	-0.586	-0.567	0.234	1.024	1.034	0.811	0.815	636
809	0.363	-0.754	-0.598	0.229	1.187	1.259	0.554	0.573	828
805	0.363	-0.754	-0.598	0.229	1.187	1.259	0.554	0.573	828
1412	0.366	-0.665	-0.617	0.227	1.057	1.078	0.622	0.645	771

TEST #	ϕ_{tp}	ψ'_{tp}	ψ'_{sp}	ψ'_{th}	H^*	ψ'_{tp}/ψ'_{sp}	α_{ups}	α_{avg}	p psi
766	0.367	-0.729	-0.626	0.226	1.121	1.165	0.745	0.754	696
746	0.370	-1.016	-0.651	0.223	1.418	1.561	0.367	0.420	914
808	0.376	-0.772	-0.699	0.217	1.080	1.104	0.525	0.546	835
807	0.382	-1.027	-0.743	0.211	1.298	1.383	0.470	0.500	867
1387	0.384	-0.676	-0.760	0.209	0.913	0.889	0.912	0.918	461
1389	0.387	-0.722	-0.789	0.206	0.933	0.916	0.919	0.925	458
1435	0.388	-0.751	-0.796	0.205	0.955	0.943	0.207	0.404	449
806	0.394	-1.153	-0.848	0.200	1.291	1.359	0.433	0.472	885
1388	0.395	-0.846	-0.858	0.198	0.989	0.986	0.926	0.931	461
770	0.396	-1.000	-0.868	0.197	1.124	1.153	0.802	0.808	629
299	0.398	-1.119	-0.881	0.196	1.221	1.271	0.414	0.473	970
1413	0.402	-1.020	-0.916	0.192	1.094	1.114	0.654	0.678	776
1386	0.408	-0.887	-0.975	0.186	0.925	0.910	0.930	0.935	441
803	0.411	-1.411	-1.008	0.183	1.339	1.401	0.328	0.397	917
1434	0.423	-1.022	-1.128	0.171	0.919	0.906	0.439	0.551	459
804	0.424	-1.528	-1.134	0.171	1.302	1.347	0.288	0.366	912
965	0.425	-1.019	-1.142	0.170	0.906	0.893	0.000	0.252	453
817	0.427	-1.047	-1.162	0.168	0.914	0.901	0.980	0.981	301
819	0.440	-1.254	-1.305	0.156	0.965	0.961	0.989	0.990	300
964	0.441	-1.178	-1.327	0.154	0.900	0.888	0.043	0.306	454
963	0.442	-1.163	-1.328	0.154	0.889	0.876	0.218	0.417	452
1410	0.443	-1.066	-1.343	0.152	0.814	0.793	0.806	0.817	539
820	0.453	-1.551	-1.469	0.142	1.051	1.056	0.992	0.993	304

C.2. Second-Quadrant Data

TEST #	ϕ_{tp}	ψ'_{tp}	ψ'_{sp}	ψ'_{th}	H^*	ψ'_{tp}/ψ'_{sp}	α_{ups}	α_{avg}	p psi
1478	-0.005	0.497	0.526	0.360	0.827	0.945	0.200	0.275	844
1480	-0.021	1.525	0.518	0.412	10.516	2.943	0.829	0.862	823
1479	-0.022	1.468	0.518	0.414	10.142	2.833	0.814	0.851	840
1476	-0.024	0.654	0.518	0.421	2.390	1.261	0.384	0.505	979
1475	-0.026	0.713	0.519	0.429	3.164	1.375	0.464	0.560	978
1474	-0.027	0.744	0.519	0.430	3.543	1.434	0.466	0.560	978
1473	-0.028	0.758	0.519	0.433	3.788	1.460	0.503	0.593	981
1477	-0.044	1.314	0.530	0.487	19.193	2.478	0.811	0.840	827
417	-0.063	0.748	0.559	0.547	17.450	1.338	0.250	0.354	992
522	-0.085	0.774	0.615	0.619	-35.646	1.258	0.035	0.108	984
418	-0.087	1.365	0.621	0.625	-161.073	2.200	0.792	0.816	984
523	-0.093	0.935	0.638	0.642	-66.388	1.466	0.372	0.444	984
437	-0.101	0.965	0.666	0.667	-170.344	1.450	0.281	0.367	976
538	-0.135	1.136	0.822	0.778	8.179	1.383	0.092	0.260	910
506	-0.155	1.355	0.937	0.842	5.400	1.446	0.362	0.411	996
507	-0.158	1.348	0.959	0.853	4.690	1.406	0.383	0.431	989
505	-0.159	1.469	0.964	0.856	5.666	1.524	0.411	0.457	991
508	-0.171	1.479	1.045	0.895	3.879	1.415	0.385	0.469	960
439	-0.203	1.597	1.290	0.997	2.049	1.238	0.096	0.205	1159
438	-0.208	1.676	1.333	1.014	2.074	1.258	0.071	0.215	962
1471	-0.240	2.106	1.627	1.115	1.935	1.294	0.229	0.319	988
540	-0.364	3.761	3.178	1.511	1.349	1.183	0.158	0.312	902
539	-0.367	3.710	3.229	1.522	1.282	1.149	0.188	0.334	902
420	-0.402	4.861	3.797	1.636	1.492	1.280	0.390	0.437	994
1472	-0.590	8.752	7.601	2.236	1.215	1.151	0.225	0.328	971
419	-0.672	10.822	9.708	2.502	1.155	1.115	0.415	0.490	963

C.3. Third-Quadrant Data

TEST #	ϕ_{tp}	ψ'_{tp}	ψ'_{sp}	ψ'_{th}	H^*	ψ'_{tp}/ψ'_{sp}	α_{ups}	α_{avg}	p psi
425	0.079	0.209	0.166	-0.092	1.167	1.260	0.399	0.471	967
427	0.110	0.235	0.202	0.009	1.171	1.163	0.387	0.427	1002
424	0.115	0.228	0.212	0.025	1.090	1.079	0.428	0.472	978
409	0.122	0.251	0.227	0.047	1.132	1.104	0.412	0.490	960
415	0.153	0.357	0.322	0.148	1.203	1.110	0.795	0.805	991
543	0.155	0.336	0.328	0.153	1.048	1.025	0.624	0.653	884
544	0.155	0.371	0.329	0.154	1.239	1.127	0.737	0.756	828
414	0.156	0.332	0.330	0.155	1.011	1.006	0.395	0.436	988
542	0.157	0.335	0.334	0.158	1.007	1.003	0.318	0.401	892
413	0.162	0.319	0.355	0.175	0.800	0.899	0.101	0.184	984
408	0.189	0.476	0.481	0.260	0.977	0.989	0.387	0.464	968
558	0.203	0.545	0.564	0.306	0.926	0.966	0.784	0.802	525
406	0.211	0.608	0.616	0.332	0.971	0.987	0.791	0.800	987
517	0.214	0.638	0.639	0.343	0.997	0.999	0.950	0.955	995
426	0.214	0.620	0.637	0.342	0.944	0.974	0.586	0.605	990
405	0.221	0.671	0.684	0.364	0.960	0.981	0.398	0.438	974
404	0.230	0.720	0.755	0.394	0.903	0.954	0.220	0.286	983
403	0.232	0.666	0.769	0.400	0.721	0.866	0.041	0.130	990
423	0.235	0.708	0.789	0.409	0.785	0.896	0.139	0.219	978

BIBLIOGRAPHY

- Chan, T.S., Investigation of Analytical Models to Correlate Centrifugal Pump Performance in Two-Phase Flow, S.M. Thesis, Massachusetts Institute of Technology, May 1977.

- Church, A.H., Centrifugal Pumps and Blowers, John Wiley & Sons, New York, 1944.

- Fishburn, J.D., et al., Two-Phase Pump-Performance, Pump-Test Facility Description, prepared by Combustion Engineering, Inc., EPRI NP-175, November 1976.

- Furuya, O., Development of an Analytic Model to Determine Pump Performance Under Two-Phase Flow Conditions, prepared by Tetra Tech, Inc., EPRI NP-3519, May 1984.

- Kennedy, W.G., et al., Pump Two-Phase Performance Program, prepared by Combustion Engineering, Inc., Vol. I,II,V,VII, EPRI NP-1556, September 1980.

- Manzano-Ruiz, J.J., Experimental and Theoretical Study of Two-Phase Flow in Centrifugal Pumps, Ph.D. Thesis, Massachusetts Institute of Technology, August 1980.

- Mikielewicz, J., et al., "A Method for Correlating the Characteristics of Centrifugal Pumps in Two-Phase Flow," Journal of Fluid Engineering, Vol. 100, 1978, pp. 395-409.

- Murakami, M., and K. Minemura, "Effects of Entrained Air on the Performance of a Horizontal Axial-Flow Pump," Polyphase Flow in Turbomachinery, ASME, New York, 1978, pp. 171-184.

- Noorbakhsh, A., Theoretical and Real Slip Factor in Centrifugal Pumps, von Karman Institute for Fluid Mechanics, technical note 93, December 1973.

- Paik, C.Y., Use of Centrifugal Pump Performance Information to Characterize a Two-Phase Flow, S.M. Thesis, Massachusetts Institute of Technology, August 1982.

- Paran, A.P., First-Quadrant Two-Phase Flow in a Vertical-Inlet Centrifugal Pump, S.M. Thesis, Massachusetts Institute of Technology, May 1983.

- Patel, B.R., and P.W. Rundstadler, Jr., "Investigations into the Two-Phase Flow Behavior of Centrifugal Pumps," Polyphase Flow in Turbomachinery, ASME, New York, 1978, pp. 79-100.

Runstadler, P.W., Jr., and F.X. Dolan, 1/20 Scale Model Pump Test Program Facility Description Report, prepared by Creare, Inc., EPRI NP-293, November 1977.

- Runstadler, P.W., Jr., and F.X. Dolan, "Two-Phase Flow, Pump Data for a Scale Model NSSS Pump," Polyphase Flow in Turbomachinery, ASME, New York, 1978, pp. 65-77.

- Stepanoff, A.J., Centrifugal and Axial Flow Pumps, John Wiley & Sons, New York, 1957.

- Stodola, A., Steam and Gas Turbines, McGraw-Hill, New York, 1927, pp. 1252-70.

- Thom, J.R.S., "Prediction of Pressure Drop During Forced Circulation Boiling of Water," International Journal of Heat and Mass Transfer, Vol. 7, Pergamon Press, New York, 1964, pp. 709-724.

- Wilson, D.G., et al., Analytical Models and Experimental Studies of Centrifugal-Pump Performance in Two-Phase Flow, prepared by Massachusetts Institute of Technology, EPRI NP-170, October 1977.

- Wilson, D.G., T. Chan, and J. Manzano-Ruiz, Analytical Models and Experimental Studies of Centrifugal-Pump Performance in Two-Phase Flow, prepared by Massachusetts Institute of Technology, EPRI NP-677, May 1979.